

AD-A089 283

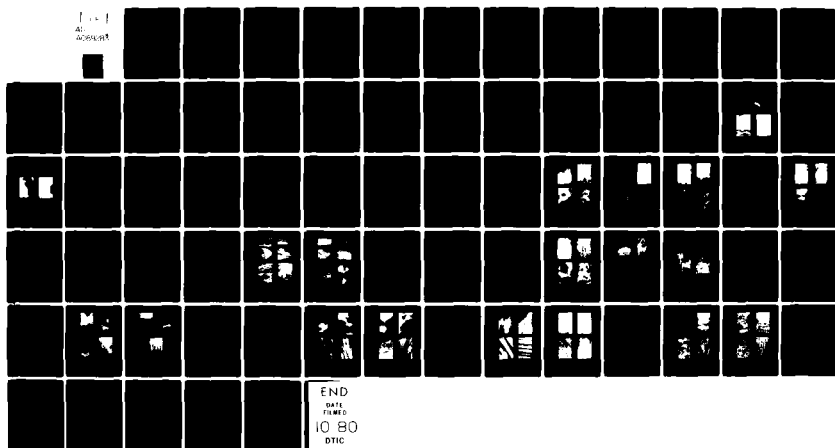
NAVAL POSTGRADUATE SCHOOL MONTEREY CA  
PRECIPITATION, RECOVERY AND RECRYSTALLIZATION UNDER STATIC AND --ETC(U)  
MAR 80 C W CHESTERMAN

F/6 11/6

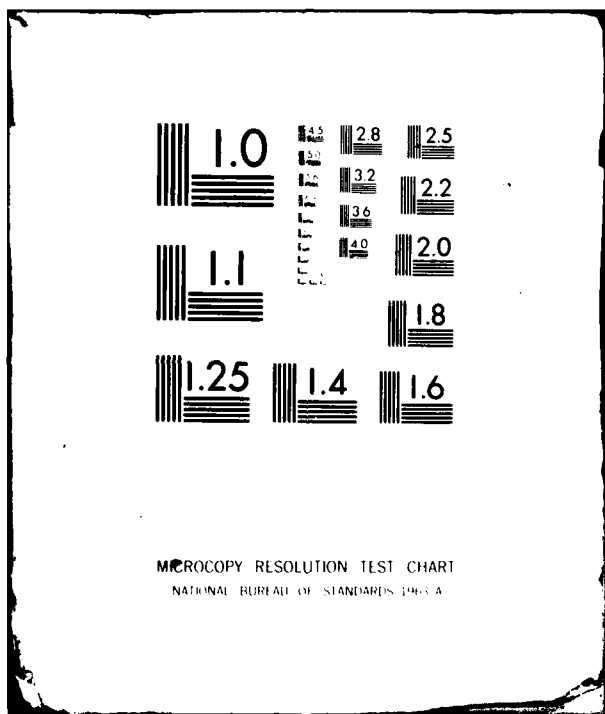
NL

UNCLASSIFIED

100%  
ALL  
INFORMATION



END  
DATE  
FILED  
10 80  
DTIC



AD A 089283

NAVAL POSTGRADUATE SCHOOL  
Monterey, California



THESIS,

Precipitation, Recovery and  
Recrystallization Under Static and Dynamic  
Conditions for High Magnesium  
Aluminum-Magnesium Alloys.

by

Charles Wesley / Chesterman, Jr.

11 Mar 1980

Thesis Advisor:

T. R. McNelley

Approved for public release; distribution unlimited

DDC FILE COPY

DTIC  
COLLECTED  
SEP 19 1980

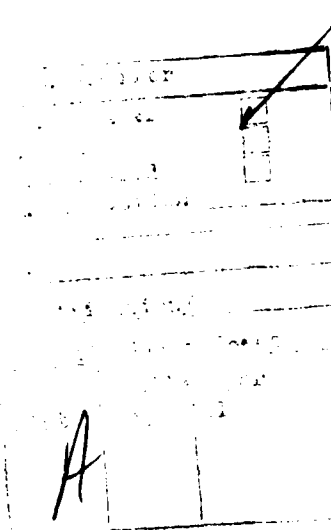
A

80 9 18 006

REPORT DOCUMENTATION PAGE		READ INSTRUCTIONS BEFORE COMPLETING FORM
1. REPORT NUMBER	2. GOVT ACCESSION NO.	3. RECIPIENT'S CATALOG NUMBER
AD-A089 283		
4. TITLE (and Subtitle) Precipitation, Recovery and Recrystallization Under Statics and Dynamic Conditions for High Magnesium Aluminum-Magnesium Alloys		5. TYPE OF REPORT & PERIOD COVERED Master's Thesis: MARCH 80
7. AUTHOR(s) Charles Wesley Chesterman, Jr.		6. PERFORMING ORG. REPORT NUMBER
9. PERFORMING ORGANIZATION NAME AND ADDRESS Naval Postgraduate School Monterey, California 93940		10. PROGRAM ELEMENT, PROJECT, TASK AREA & WORK UNIT NUMBERS
11. CONTROLLING OFFICE NAME AND ADDRESS Naval Postgraduate School Monterey, California 93940		12. REPORT DATE March 1980
14. MONITORING AGENCY NAME & ADDRESS/If different from Controlling Office) Naval Postgraduate School Monterey, California 93940		13. NUMBER OF PAGES 72
15. SECURITY CLASS. (of this report) Unclassified		
16. DECLASSIFICATION/DOWNGRADING SCHEDULE		
17. DISTRIBUTION STATEMENT (of this Report) Approved for public release; distribution unlimited		
18. DISTRIBUTION STATEMENT (of the abstract entered in Block 20, if different from Report)		
19. SUPPLEMENTARY NOTES		
20. KEY WORDS (Continue on reverse side if necessary and identify by block number)		
21. ABSTRACT (Continue on reverse side if necessary and identify by block number) Previous studies of the mechanical behavior of warm rolled high magnesium aluminum-magnesium alloys have shown that excellent tensile properties can be developed in these materials. Several questions raised in these previous efforts regarding recrystallization and precipitation of the intermetallic $\beta$ phase are addressed in this thesis. It is shown that, for temperatures $T < T_s$ (where $T_s$ is the solvus temperature) the only microstructural change is		

the precipitation of the  $\beta$  phase and no crystallization occurs, even with prior cold work. Further studies of microstructures developed during warm working, with and without prior cold work, also indicate that precipitation and recovery dominate the microstructural changes in warm rolling at temperatures below the solvus for the alloy. Recrystallization will occur readily, but only at temperature in excess of the solvus. Strengthening by warm working, then, occurs by mechanisms similar to cold work strengthening in solid solution alloys.

11



Approved for public release; distribution unlimited

Precipitation, Recovery and Recrystallization  
Under Static and Dynamic Conditions  
for High Magnesium Aluminum-Magnesium Alloys

by

Charles Wesley Chesterman, Jr.  
Lieutenant, United States Navy  
B.S., United States Naval Academy, 1974

Submitted in partial fulfillment of the  
requirement for the degree of

MASTER OF SCIENCE IN MECHANICAL ENGINEERING

from the

NAVAL POSTGRADUATE SCHOOL  
March 1980

Author

Charles Wesley Chesterman

Approved by:

Henry R. McNelley Thesis Advisor

James S. Collier Second Reader

B. J. Marks  
Chairman, Department of Mechanical Engineering

William M. Jolley  
Dean of Science and Engineering

## ABSTRACT

Previous studies of the mechanical behavior of warm rolled high magnesium aluminum-magnesium alloys have shown that excellent tensile properties can be developed in these materials. Several questions raised in these previous efforts regarding recrystallization and precipitation of the intermetallic  $\beta$  phase are addressed in this thesis. It is shown that, for temperatures  $T < T_s$  (where  $T_s$  is the solvus temperature) the only microstructural change is the precipitation of the  $\beta$  phase and no recrystallization occurs, even with prior cold work. Further studies of microstructures developed during warm working, with and without prior cold work, also indicate that precipitation and recovery dominate the microstructural changes in warm rolling at temperatures below the solvus for the alloy. Recrystallization will occur readily, but only at temperature in excess of the solvus. Strengthening by warm working, then, occurs by mechanisms similar to cold work strengthening in solid solution alloys.

## TABLE OF CONTENTS

I.	INTRODUCTION-----	11
	A. BACKGROUND-----	11
	B. PHYSICAL AND MECHANICAL PROPERTIES-----	12
	C. PREVIOUS WORK-----	17
	D. PURPOSE OF THESIS-----	18
II.	PROCESSING PROCEDURES AND EXPERIMENTAL METHODS-----	19
	A. PROCESSING AND MECHANICAL TESTING EQUIPMENT-----	19
	B. METALLOGRAPHY-----	20
	C. MATERIAL PROCESSING-----	21
III.	PRECIPITATION STUDY-----	27
	A. PROCEDURE-----	27
	B. HARDNESS AS A FUNCTION OF TIME AND TEMPERATURE-----	27
	C. MICROSTRUCTURE AS A FUNCTION OF TIME AND TEMPERATURE-----	34
	D. CONCLUSIONS-----	38
IV.	RECRYSTALLIZATION AND RECOVERY IN ALUMINUM-8% MAGNESIUM-----	41
	A. BACKGROUND-----	41
	B. PROCEDURE-----	43
	C. RESULTS AND DISCUSSION-----	44
V.	DYNAMIC STUDY OF ALUMINUM-8% MAGNESIUM-----	53
	A. BACKGROUND-----	53
	B. PROCEDURE-----	53
	C. COLD WORKING-----	54
	D. COLD ROLLING FOLLOWED BY WARM ROLLING AT 300° C-----	58

E. WARM ROLLING AT 300° C -----	61
F. COLD ROLLING FOLLOWED BY WARM ROLLING AND WARM ROLLING AT 340° C-----	64
G. SUMMARY AND CONCLUSIONS-----	64
VI. CONCLUSIONS AND RECOMMENDATIONS-----	70
LIST OF REFERENCES-----	71
INITIAL DISTRIBUTION LIST-----	72

## LIST OF FIGURES

Figure 1. A partial Aluminum-Magnesium phase diagram. Compositions are indicated with dashed lines, temperatures are indicated by dot-dashed lines.---22

Figure 2. Micrograph (a) shows dendritic non-homogeneous as-cast structure of a 14% Mg alloy. Micrographs (b) and (c) are solution treated 20 hours at  $450^{\circ}\text{C}$  and air cooled and oil quench respectively, 100X.---24

Figure 3. Micrographs (a) and (b) are 14% Mg alloy solution treated 20 hours at  $450^{\circ}\text{C}$ , forged, solution treated 4 hours at  $450^{\circ}\text{C}$ , air cooled and oil quench respectively, 100X.-----26

Figure 4. Precipitation Study at  $125^{\circ}\text{C}$ , plot of hardness, Rockwell Scale "B" as a function of time.-----28

Figure 5. Precipitation Study at  $200^{\circ}\text{C}$ , plot of hardness, Rockwell Scale "B" as a function of time.-----29

Figure 6. Precipitation Study at  $300^{\circ}\text{C}$ , plot of hardness, Rockwell Scale "B" as a function of time.-----30

Figure 7. Precipitation Study at  $340^{\circ}\text{C}$ , plot of hardness, Rockwell Scale "B" as a function of time.-----31

Figure 8. Precipitation Study at  $380^{\circ}\text{C}$ , plot of hardness, Rockwell Scale "B" as a function of time.-----32

Figure 9. Precipitation Study at  $420^{\circ}\text{C}$ , plot of hardness, Rockwell Scale "B" as a function of time.-----33

Figure 10. Micrographs (a), (b), (c) and (d) Precipitation Study of 8% Mg alloy, 50 minutes at temperatures  $125^{\circ}\text{C}$ ,  $200^{\circ}\text{C}$ ,  $300^{\circ}\text{C}$ , and  $340^{\circ}\text{C}$  respectively, 40X.-----35

Figure 11. Micrographs (a), (b), (c) and (d) Precipitation Study of 8% Mg alloy, 8 hours and 20 minutes at temperatures  $125^{\circ}\text{C}$ ,  $200^{\circ}\text{C}$ ,  $300^{\circ}\text{C}$ , and  $340^{\circ}\text{C}$  respectively, 160X.-----36

Figure 12. Micrographs (a) and (c) Precipitation Study of 14% Mg Alloy, 20 minutes at temperatures  $125^{\circ}\text{C}$  and  $200^{\circ}\text{C}$  respectively. Micrographs (b) and (d) Precipitation Study of 14% Mg Alloy, 50 minutes at temperatures  $125^{\circ}\text{C}$  and  $200^{\circ}\text{C}$  respectively, 40X.-----37

Figure 13. Micrographs (a) and (b) Precipitation Study of 14% Mg alloy at 300° C for 20 and 50 minutes respectively. Micrographs (c) and (d) Precipitation Study of 14% Mg alloy at 340° C for 20 and 50 minutes respectively, 40X.-----39

Figure 14. Micrographs (a), (b), (c) and (d) Recrystallization Study of 8% Mg alloy, 50 minutes at temperatures 125° C, 200° C, 300° C and 340° C respectively, 40X.-----44

Figure 15. Micrographs (a), (b), (c) and (d) Recrystallization Study of 8% Mg alloy, 8 hours and 20 minutes at temperatures 125° C, 200° C, 300° and 340° C respectively, 160X.-----45

Figure 16. Recrystallization Study of 8% Mg alloy, plot of hardness, Rockwell Scale "B" as a function of time for deformation temperature of 125° C.-----47

Figure 17. Recrystallization Study of 8% Mg alloy, plot of hardness, Rockwell Scale "B" as a function of time for deformation temperature of 20° C.-----48

Figure 18. Micrographs (a) and (b) Recrystallization Study of 8% Mg alloy, 8 hours and 20 minutes at 340° C and 380° C respectively, 40X. Micrographs (c) and (d) Recrystallization Study of 8% Mg alloy, 8 hours and 20 minutes at 340° C and 380° C respectively, 160X.-----49

Figure 19. Micrographs (a) and (b) Recrystallization Study of 8% Mg alloy, at 340° C for 10 and 50 minutes respectively, 40X. Micrographs (c) and (d) Recrystallization Study of 8% Mg alloy, at 340° C for 10 and 50 minutes respectively, 160X.-----50

Figure 20. Micrographs (a) and (b) Recrystallization Study of 8% Mg alloy, at 340° C for 10 minutes and 1 hour and 40 minutes respectively, 40X.-----51

Figure 21. Micrographs (a), (b), (c) and (d) Dynamic Study of 8% Mg alloy cold rolling sequence, cumulative rolling strain of .01, .05, .17 and .83 respectively, 40X.-----55

Figure 22. Micrographs (a), (b) and (c) Dynamic Study of 8% Mg alloy cold rolling sequence, cumulative rolling strain of 1.19, 1.85 and 2.96 respectively, 40X.-----56

Figure 23. Dynamic Studu of 8% Mg alloy, plot of hardness, Rockwell Scale "B" as a function of cumulative strain for cold, cold/warm and warm rolling sequences.-----57

Figure 24. Micrographs (a), (b), (c) and (d) 300° C Dynamic Study of 8% Mg alloy cold/warm rolling sequence, cumulative rolling strain of .33, .78, 1.37 and 2.47 respectively for 70 minutes at temperature, 40X.-----59

Figure 25. Micrographs (a), (b), (c) and (d) 300° C Dynamic Study of 8% Mg alloy cold/warm rolling sequence, cumulative rolling strain of .28, .76, 1.08, and 2.16 respectively for 210 minutes at temperature, 40X.-----60

Figure 26. Micrographs (a), (b), (c) and (d) 300° C Dynamic Study of 8% Mg alloy warm rolling sequence, cumulative rolling strain of .35, .80, 1.37 and 2.45 for 70 minutes at temperature, 40X.-----62

Figure 27. Micrographs (a), (b), (c) and (d) 300° C Dynamic Study of 8% Mg alloy warm rolling sequence, cumulative rolling strain of .26, .78, 1.08 and 2.19 respectively for 210 minutes at temperature, 40X.-----63

Figure 28. Micrographs (a), (b), (c) and (d) 340° C Dynamic Study of 8% Mg alloy cold/warm rolling sequence, cumulative rolling strain of .31, .83, 1.39 and 2.02 respectively for 70 minutes at temperature, 40X.-----65

Figure 29. Micrographs (a), (b), (c) and (d) 340° C Dynamic Study of 8% Mg alloy warm rolling sequence, cumulative rolling strain of .33, .86, 1.4 and 2.03 respectively for 70 minutes at temperature, 40X.-----66

## LIST OF TABLES

Table I	Mechanical Properties of Several Principal Aluminum Alloys as 1/16 In-Thick Sheet (Adapted from Ref. 2)-----	13
Table II	Density of Selected Aluminum Alloys (Adapted from Ref. 2)-----	16
Table III	Recrystallization Temperature Calculated for Various High Magnesium Aluminum Alloys (Adapted from Ref. 2)-----	42
Table IV	Table of Thermomechanical Processing Mechanical Testing Results (8% Magnesium Alloy)-----	69

## I. INTRODUCTION

### A. BACKGROUND

The industrial use of aluminum and its many alloys is exceeded only by that of steel amongst metallic materials. Aluminum first became commercially available less than one hundred years ago and its usage is sure to increase in the future. Insights into its behavior and capabilities will only expand its usage as man uses this knowledge to overcome the difficulties and disadvantages of this metal and its alloys.

With a density of  $.0975 \text{ lb/in}^3$  ( $2.7 \text{ gm/cm}^3$ ), aluminum is about one third the density of iron; this leads to structural weight reduction especially important in aircraft, automotive and other transportation industries where performance and 'miles-per-gallon' are of prime importance. [Ref. 1] The strength and hardness of aluminum alloys will not approach that of the highest strength steels, but many aluminum alloys equal or exceed the strength and ductility of many structural steels. At subzero temperatures, the strength and ductility of aluminum increases, contrary to many steels which become increasingly brittle. On the other hand, the maximum useful temperature for the most heat resistant aluminum alloys is  $500^\circ \text{ F}$  ( $260^\circ \text{ C}$ ). [Ref. 1,2]

The rapid formation of aluminum oxide and its adherance and self-limiting character makes aluminum alloys an excellent selection in some corrosive environments. Likewise the similar electro-chemical activity and inherently higher strength of

aluminum alloys make them more useful than zinc alloys as a sacrificial anodes for ship hull protection. [Ref. 1] The face-centered cubic crystal structure of aluminum lends itself to excellent ductility and thus ease of forming for many of its alloys. Also, aluminum may be formed at ambient temperatures with low power equipment in contrast to steels, which present more difficulties in manufacture. [Ref. 1] The electrical and thermal properties of aluminum make it very suitable for power transmission and for use in heating and cooling applications, especially when coupled with its light weight and high strength.

#### B. PHYSICAL AND MECHANICAL PROPERTIES

The addition of various alloying elements (copper, manganese, silicon, magnesium and zinc), in varying amounts, increase strength while retaining the attribute of low density in the alloy. [Ref. 3] To distinguish between the various alloys, they are grouped by the major alloying element. Each major alloying element has an identifying series number: copper (2xxx), manganese (3xxx), silicon (4xxx), magnesium (5xxx), magnesium and silicon (6xxx), zinc (7xxx), and other elements (8xxx). This identification system is applicable to wrought alloys and only the wrought alloys will be discussed here. [Ref. 1,2] The composition and tensile properties of several common wrought aluminum alloys are given in Table I.

The wrought alloys are placed into two general categories: heat treatable and non-heat treatable. The alloys that are

Table I  
Mechanical Properties of Several Principal Aluminum  
Alloys as 1/16 In-Thick Sheet (Adapted from Reference 2)

Alloy	Composi- tion, %	Temper	Tensile Strength $10^3$ lb/in $^2$ (MPa)	0.2% Yield Strength $10^3$ lb/in $^2$ (MPa)	Elonga- tion in 2 in. %
<u>Non-Heat Treatable</u>					
1100	99.00 Al	-0	13 (89.6)	5 (34.5)	35
		-H14*	18 (124.0)	17 (117.1)	9
		-H18	24 (165.4)	22 (151.6)	5
3003	1.2 Mn	-0	16 (110.2)	6 (41.3)	30
		-H14	21 (144.6)	8 (55.1)	16
		-H18	29 (199.8)	27 (185.0)	4
3004	1.2 Mn 1.0 Mg	-0	26 (179.1)	10 (68.9)	20
		-H14	35 (241.1)	29 (199.8)	9
		-H18	41 (282.5)	36 (248.0)	5
5052	2.5 Mg 0.2 Cu	-0	28 (192.9)	13 (89.6)	30
		-H34	38 (261.8)	31 (213.6)	14
		-H38	42 (289.4)	37 (254.9)	8
5056	5.2 Mg 0.1 Mn 0.1 Cr	-0	42 (289.4)	22 (151.6)	35
		-H18	63 (434.0)	59 (406.5)	10
		-H38	60 (413.4)	50 (344.5)	15
<u>Heat Treatable</u>					
2014	4.4 Cu 0.8 Si 0.4 Mg 0.4 Mg	-0	27 (186.0)	14 (96.5)	22
		-T4**	63 (434.0)	40 (275.6)	18
		-T6	70 (482.3)	60 (413.4)	10
2024	4.5 Cu 0.6 Mn 1.0 Mg	-0	27 (186.0)	11 (75.8)	20
		-T4	68 (468.5)	47 (323.8)	20
		-T6	70 (482.3)	60 (413.4)	10
		-T86	75 (516.7)	71 (489.2)	6
6061	1.0 Mg 0.6 Si 0.2 Cr	-0	18 (124.0)	8 (55.1)	75
		-T4	35 (241.1)	21 (144.7)	25
		-T6	45 (310.1)	40 (275.6)	12
		-T91	59 (406.5)	57 (392.7)	6
7075	5.5 Zn 2.5 Mg 1.5 Cu 0.3 Cr	-0	33 (227.3)	15 (103.4)	17
		-T6	83 (571.8)	73 (502.9)	11

\* The Temper H refers to the properties after cold working.

\*\* The Temper T refers to the properties after aging.

heat treatable are the 2xxx, 6xxx and 7xxx series. The alloys that are work hardenable are the 3xxx and 5xxx series. The heat treatable alloys gain their strength and hardness from solid solution strengthening and precipitation hardening while the non-heat treatable alloys are strengthened by solid solution strengthening and cold work. [Ref. 1,2,3]

Precipitation hardening is a two-part process. The first part involves a solution treatment wherein the alloy is heated to a temperature sufficient to dissolve the second phase in the primary phase. It is then rapidly quenched, the speed of the quench preventing the formation of equilibrium precipitates; thus, a supersaturated solid solution is obtained. [Ref. 1,4,5] The second part of the precipitation process is the aging treatment, which involves the nucleation and growth of a second phase. Nucleation begins after a finite time called the incubation period where stable nuclei are formed. Nucleation may be either heterogeneous or homogeneous. The formation of nuclei at lattice defects, e.g. slip planes, grain boundaries and inclusions, is heterogeneous. The spontaneous formation of the second phase in the lattice is homogeneous nucleation. [Ref. 4,5] Following nucleation, growth occurs; precipitate particles eventually attain a size and number sufficient to impede dislocation motion and thus strengthen the alloy.

Cold working of a non-heat treatable alloy is accomplished by rolling, drawing, forging or extruding at ambient temperatures. Strengthening during cold work results from an increased density

of dislocations. In addition, alloying elements in solid solution interact with dislocations in the material further impeding their motion. In general, the non-heat treatable aluminum alloys are lower in strength than heat treatable alloys.

Dispersion hardening is similar to precipitation hardening in that the strengthening is due to a second phase. The difference is that the particles in dispersion hardening are insoluble and generally more widely dispersed within the material and thus are less influenced by prolonged exposure to elevated temperature. The precipitation-hardening particles, on the other hand, have a transition structure related to the aging time. There can be a loss in hardness due to prolonged time at temperature and this is called overaging. [Ref. 5]

Magnesium is a preferred alloying element in many commercial aluminum alloys. Magnesium is more soluble in solid solution than any other element used as a solid solution strengthener in aluminum. In the marine environment, magnesium-containing alloys have excellent corrosion resistance as well as fatigue and shock resistance. Magnesium-containing alloys also have excellent forming and welding characteristics. [Ref. 1] Magnesium presently is the only alloying element commercially used in aluminum that is less dense than aluminum. In alloying aluminum with magnesium, the resulting alloy is less dense than pure aluminum. Densities of several common commercial alloys are listed in Table II.

Table II  
Densities of Selected Aluminum Alloys  
(Adapted from Reference 2)

<u>ALLOY DESIGNATION</u>	<u>DENSITY, GRAMS PER CM<sup>3</sup></u>
1100	2.71
2014	2.80
2024	2.77
3003	2.73
5052	2.68
5056	2.64
6061	2.71
7075	2.80

### C. PREVIOUS WORK

The previous work on high magnesium aluminum-magnesium alloys conducted at the Naval Postgraduate School was done by Ness [Ref. 6], Bingay [Ref. 7], Glover [Ref. 8], Grandon [Ref. 9] and Speed [Ref. 10]. These previous studies investigated magnesium contents from 7% to 20% and focused on various techniques of refining the microstructure of the as-cast material.

Ness observed that slow rolling of an 18% magnesium alloy lead to microstructural refinement and that the material strain hardened quite rapidly during ambient temperature testing. An attempt was made to use a more rapid rolling or forging process, but this was only successful on alloys containing less than the maximum solubility of magnesium in aluminum. Bingay experimented with upset forging, Grandon utilized solution treatment and Speed combined upset forging with solution treatment and warm isothermal rolling. With alloys up to 10% magnesium, processing can be readily accomplished, producing tensile strengths up to 82 KSI (56.5 MPa), yield strengths up to 65 KSI (44.8 MPa), and an elongation of 11%.

The possibility of developing high strength alloys was well established by the previous work. A recurrent question raised by the previous work in this area is: what is the role of precipitation and role of recrystallization in the development of the microstructures during thermal mechanical processing of these alloys? It was assumed that recrystallization would occur during warm working leading to a refined grain structure

and homogeneous dispersion of the precipitating intermetallic  $\beta$  phase,  $\text{Al}_3\text{Mg}_2$ . However, no clear evidence of recrystallization was ever obtained for rolling at temperatures substantially below the solvus temperatures for these alloys.

#### D. PURPOSE OF THESIS

The purpose of this work was to investigate the phenomena of precipitation and recrystallization and attempt to determine those thermomechanical processing conditions under which recrystallization and precipitation occur. Questions addressed were: does recrystallization occur at temperatures below the solvus for the alloy in question; also, does it occur before precipitation, or at all during warm rolling, i.e. at temperatures below the solvus?

The study was structured to investigate precipitation and recrystallization under 'static' conditions, wherein these processes are examined during a simple annealing of the alloy, and under 'dynamic' conditions where the material was warm worked at the temperature in question.

## II. PROCESSING PROCEDURES AND EXPERIMENTAL METHODS

### A. PROCESSING AND MECHANICAL TESTING EQUIPMENT

Materials were solution treated in a Lindburg Heavy Duty Stable-Glow box type furnace with a proportional control system. Forging was accomplished using a Baldwin-Tate-Emery Tensile Machine that was modified to utilize heated plattens with a proportional control heating system manufactured at the Naval Post-graduate School. All rolling was done on a 2-high, variable speed rolling mill, Fenn Model 172. The mill has a maximum roll gap of 1.25 inches (32 mm). The roll diameter is 4.25 inches (108 mm) and width is 6.0 inches (152 mm). During isothermal rolling, the material was initially heated and reheated after each pass in a Blue M Model 8655F-3 Stable Glow box type furnace, with a proportional control system.

Precipitation and recrystallization study samples were cut from forged blocks on a band saw. Surfaces of the blanks were ground flat utilizing a Buehler duo belt wet surfacer. Hardness testing was done on a Wilson Model 1JR Rockwell Hardness Tester using a Rockwell "B" scale. Tensile testing was done on a Model TT-D Instron Floor Model Testing Machine. A constant crosshead speed of .05 inches per minute (1.27 mm/min) was used for all testing. Specimen blanks for tensile testing 5.0 x .75 inches (127 x 19 mm), were cut from rolled material. The tensile test specimen gage length was 2 inches. Elongation was based upon measured extension at fracture.

## B. METALLOGRAPHY

Specimens were mounted individually in 1 1/4 inch diameter Buehler quick-dry mounting cups with the buttend of the specimen protruding. After hardening and curing of the mold, the specimens were ground flat using a succession of grits with 600 wet grit being the last. Polishing was done on rotating wheels with a 0.05 mm Gamma Alumina Powder the last. Final polishing of the specimens was accomplished on a Buehler Vibromet. The mounting weights for the Vibromet were modified to hold the 1 1/4 inch diameter specimens. A micro cloth pad was used with a slurry of Magomet in the proportion of 55 grams to 250 ml of distilled water.

Four to six specimens were polished at a time with the rotation speed of the Vibromet adjusted for a slow rotation. It was found that with too high a speed, pitting would occur and with too low a speed the specimens would not polish. Time of polishing varied for each specimen and the time of polishing was dependent upon both the surface area and magnesium content. The higher the magnesium content and the larger the surface area, the more time required. An 8% magnesium alloy sample of size 12.7 x 19.9 mm took, on the average, 30 minutes. The slurry of Magomet was good for about 8 hours, after which it became too thick, leading to pitting. Specimens were cleaned in ethyl alcohol in an ultrasonic bath for approximately 10 to 15 seconds to remove any slurry prior to blow drying.

To aid in distinguishing the microstructural features, a dilute fluoroboric acid solution (Barker's Reagent) and electro

etching were used. A stainless steel disk was emersed in the dilute fluoroboric acid and connected to the cathodic lead of a Buehler Electromet Power Source. The butt end of the specimen was connected to the anode lead. A voltage setting of 30 volts was utilized. Time of immersion in the fluoroboric acid depended upon two factors: the surface area of the specimen, and the polish quality of the specimen surface. The larger the surface area and the better the polish the greater the immersion time. For a 12.7 x 19.1 mm sample, times varied from 5 to 25 seconds. Light micrographs were made on a Carl Zeiss Universal Microscope utilizing a crossed polarizer and analyzer.

#### C. MATERIAL PROCESSING

The Material used in the studies was produced by the direct-chill casting method at Alcoa Technical Center, Alcoa Center, Pennsylvania. The direct chill casting method employs a water-cooled copper mold with a retractable water-cooled copper base plate which is withdrawn as the molten metal is poured in the top. This method prevents macro-segregation but the resulting structure is dendritic and not homogeneous on a microscale.

From these cast ingots standard forging billets 1.2 x 1.2 x 3.0 inch (30.5 x 30.5 x 76.2 mm) were cut. Based on the work of Grandon [Ref. 9] and Speed [Ref. 10], a solution treatment and upset forging schedule was developed to refine the as-cast dendritic structure. Solution treatment was accomplished by heating into the single-phase  $\alpha$  region and holding for a period of time. Figure 1 is a partial aluminum-magnesium phase diagram

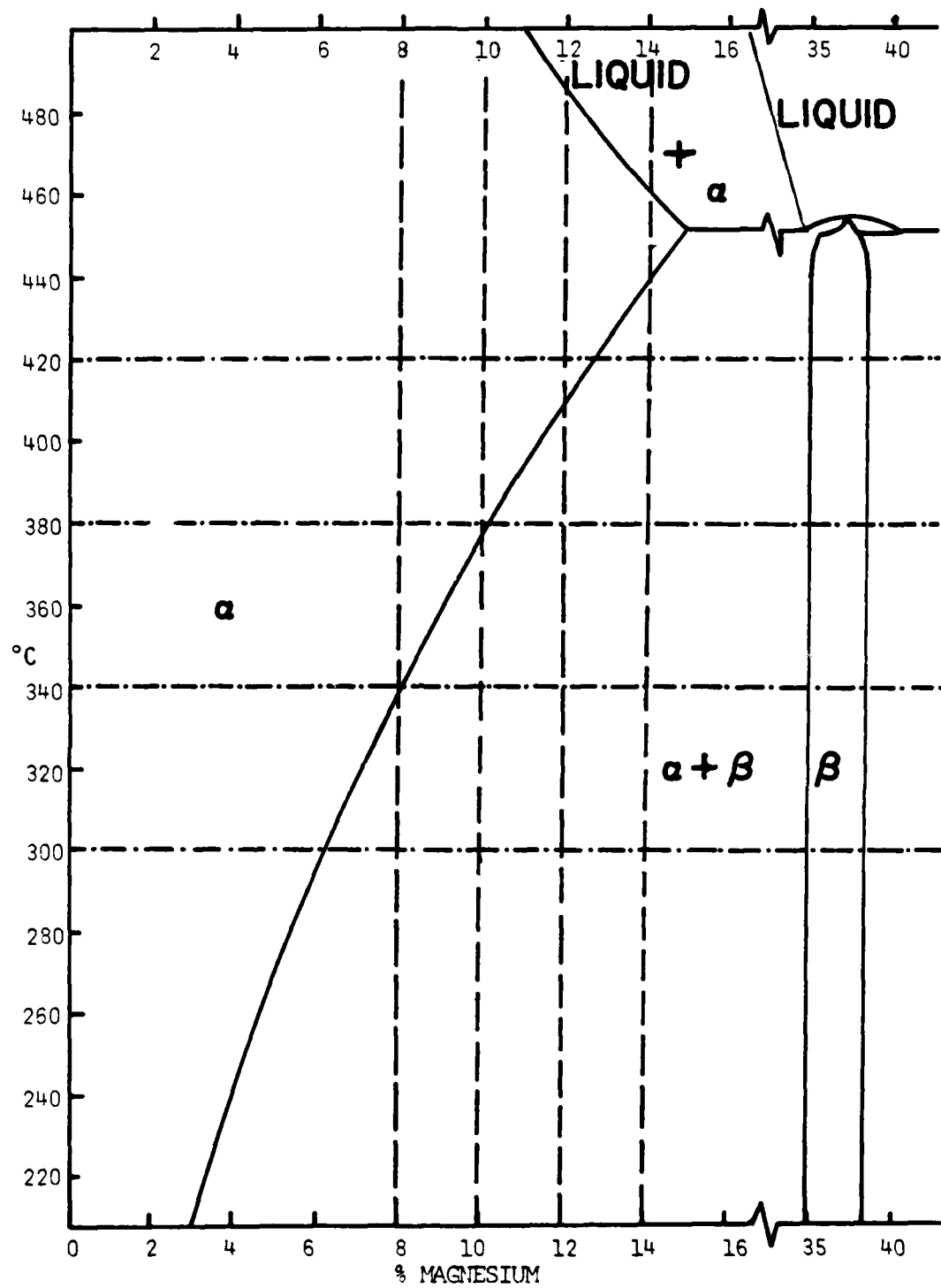


Figure 1. A partial Aluminum-Magnesium phase diagram. Compositions are indicated with dashed lines, temperatures are indicated by dot-dashed lines.

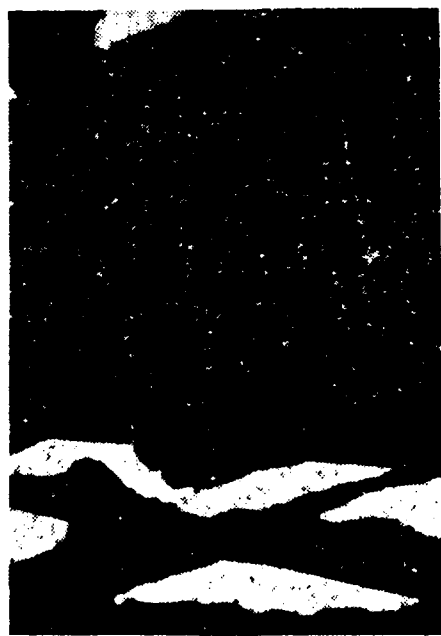
applicable to the alloys studied. The region labeled  $\alpha$  is the single-phase region where solution treatment can take place. Limitations on solution treatment are the solvus temperature for the particular alloy, and the melting temperature of the second phase, for  $\beta$ ,  $451^{\circ}\text{C}$ . Grandon [Ref. 9] found that 20 hours was sufficient time for complete solution of the  $\beta$  phase at  $440^{\circ}\text{C}$ .

A study was conducted on a 14% magnesium alloy to ascertain the proper temperature for solution treatment and the cooling rate required to preserve the microstructure obtained by the solution treatment. A temperature range of  $440^{\circ}\text{C}$  to  $450^{\circ}\text{C}$  and time of 20 hours were used. The temperature of  $450^{\circ}\text{C}$  was found to be most satisfactory. Selected micrographs from this study are shown in Figure 2. The oil quench retains the magnesium in solution better than does air cooling. The intermetallic 3 phase precipitates during air cooling and does so in a pattern suggesting the as-cast dendritic structure. This 14% magnesium alloy represents the most difficult material in which to keep the magnesium in solution. Lower magnesium alloys will have a lower solvus temperature, and thus, if an oil quench is sufficient in this alloy, it will also be sufficient for the lower magnesium alloys.

The upset forging procedure was added to achieve further refinement of the microstructure. As utilized by Speed [Ref. 10], the upset forging sample, after a 20 hour solution treatment, was placed between heated plattens and forged to a thickness of



(a)



(b)



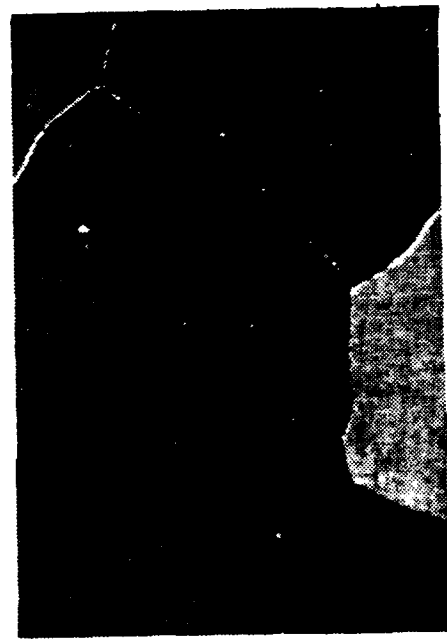
(c)

Figure 2. Micrograph (a) shows dendritic, non-homogeneous as-cast structure of a 14% Mg alloy. Micrographs (b) and (c) are solution treated 20 hours at 450° C and air cooled and oil quench respectively, 100X.

1 inch. The sample was returned to a furnace for an additional four-hour solution treatment followed by oil quenching. Figure 3 illustrates the difference between oil quenching and air cooling. Starting material for all subsequent studies was then obtained from material given the combination of solution treatment, upset forging, solution treatment and oil quenching.



(a)



(b)

Figure 3. Micrographs (a) and (b) are the 14% Mg alloy solution treated 20 hours at  $450^{\circ}\text{ C}$ , forged, solution treated 4 hours at  $450^{\circ}\text{ C}$ , and then air cooled or oil quench respectively, 100X.

### III. PRECIPITATION STUDY

#### A. PROCEDURE

The first study under was of static precipitation in alloys containing 8%, 10%, 12% and 14% magnesium. All materials were, as previously noted, from billets solution treated, forged, solution treated and oil quenched. These billets were sectioned, as previously described, and samples were then annealed for varying times at temperatures ranging from 125° C to 420° C. At the conclusion of the anneal, the samples were always oil quenched. Hardness data was obtained and the influence of time and temperature was evaluated metallographically.

#### B. HARDNESS AS A FUNCTION OF TIME AND TEMPERATURE

The hardness verses time at temperature for the various temperatures is presented in Figure 4 through Figure 9. For 125° C there is no significant change in hardness with annealing time. At 200° C, the 8% magnesium alloy maintains a fairly consistent hardness, while the 10%, 12% and in particular the 14% magnesium alloys exhibit precipitation hardening (increased hardness with increased aging time).

At 300° C, the 8% magnesium alloy shows a slight increase in hardness. The 10%, 12% and 14% magnesium alloys show precipitation hardening and the 14% magnesium alloy begins over-aging after about 50 hours. This trend is also evident for the 12% and the 14% magnesium alloys at 340° C. The 8% and 10% magnesium alloys at 340° C are showing some minimal hardening; this temperature, 340° C, is just above the solvus for the 8% magnesium alloy.

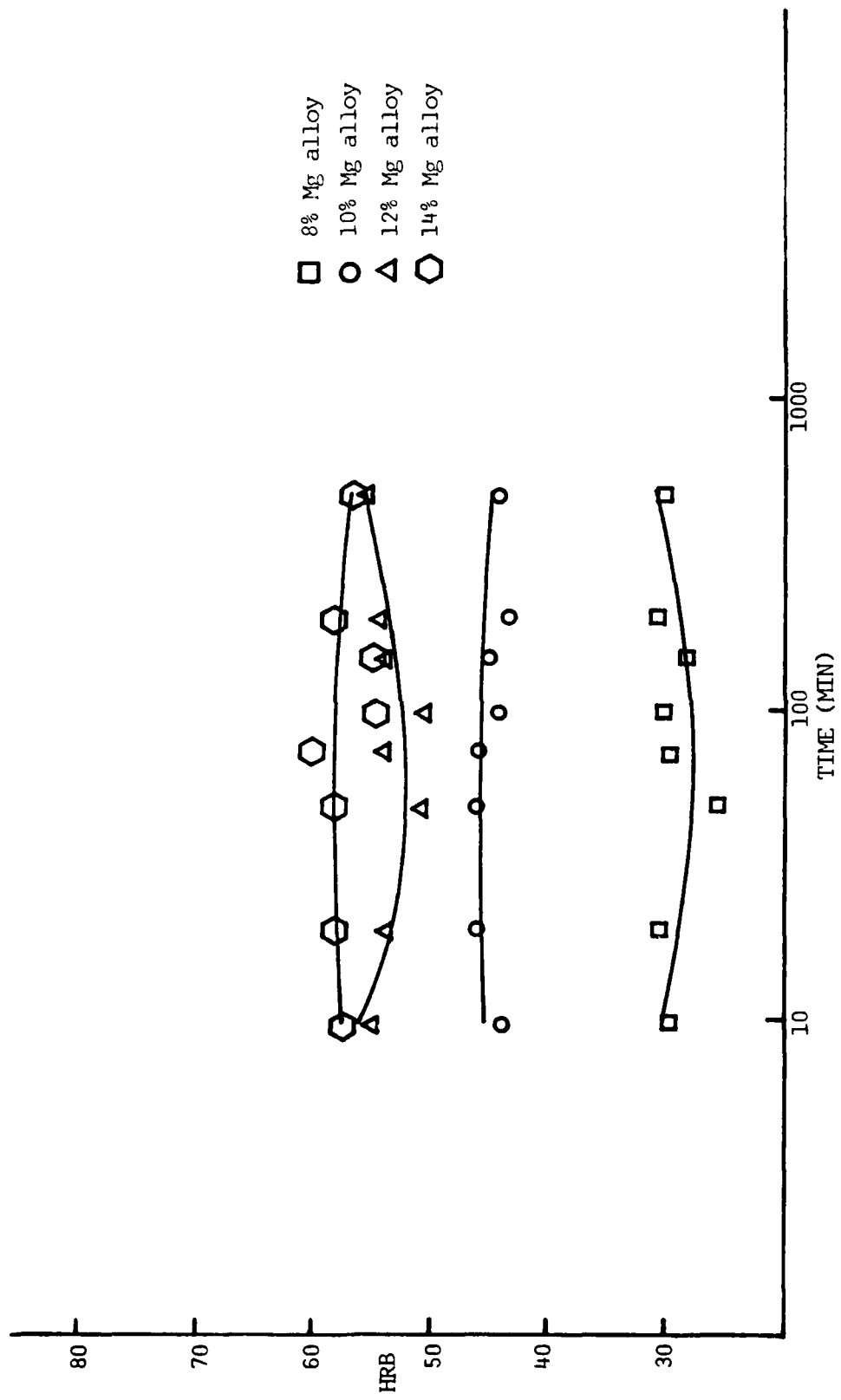


Figure 4. Precipitation Study at  $125^{\circ}\text{C}$ , plot of hardness, Rockwell Scale "B" as a function of time.

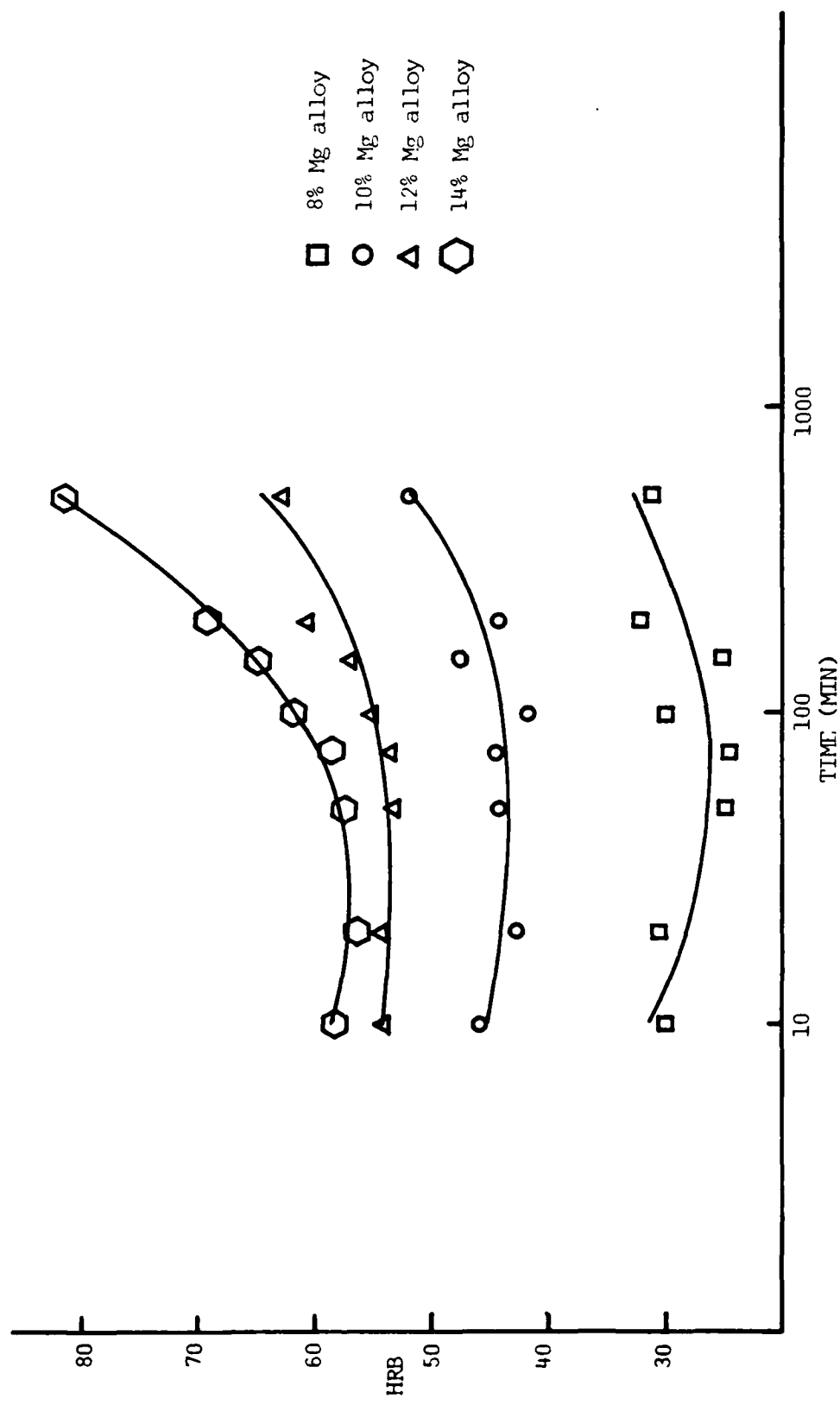


Figure 5. Precipitation Study at  $200^{\circ}\text{C}$ , plot of hardness, Rockwell Scale "B" as a function of time.

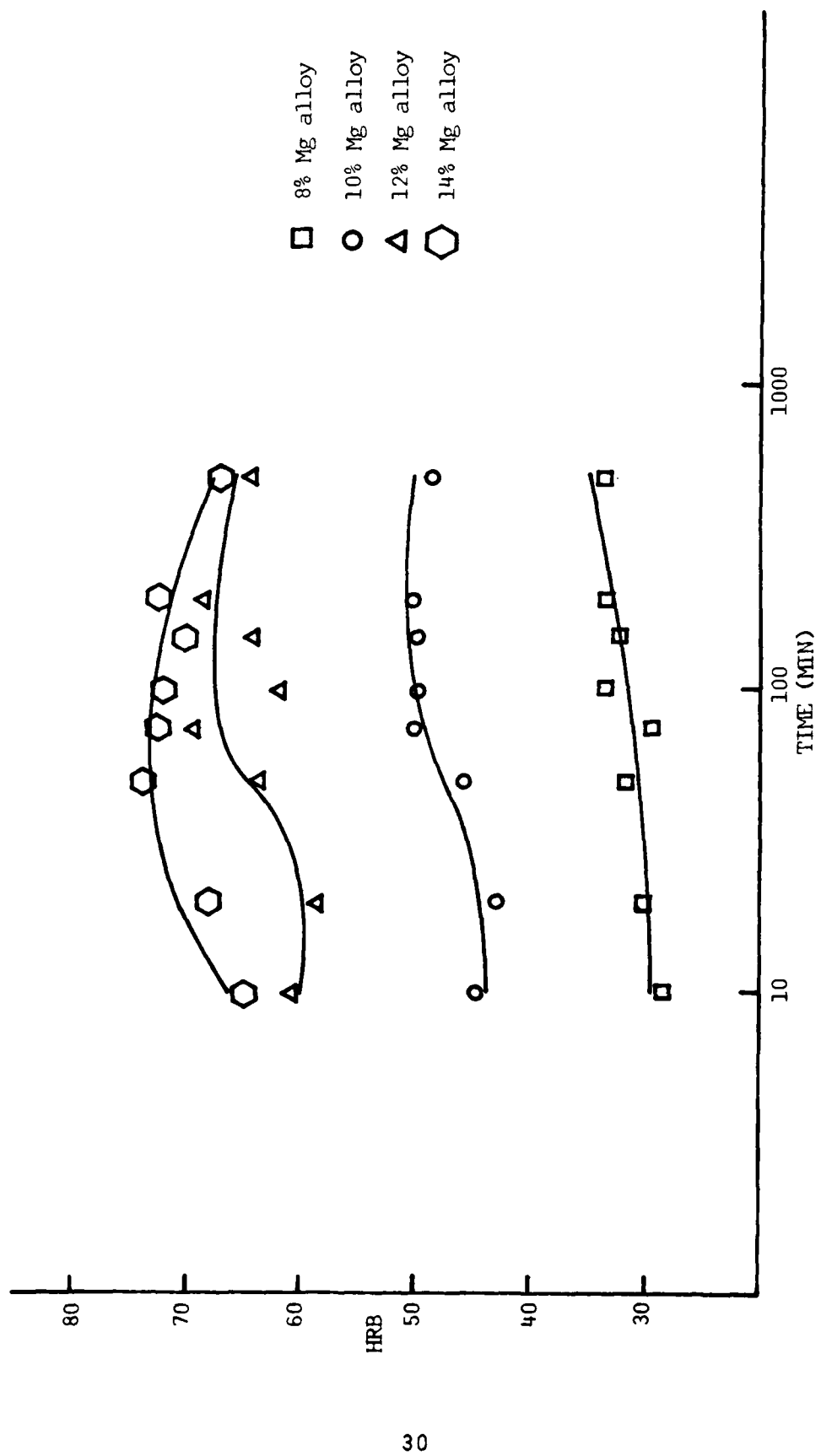


Figure 6. Precipitation Study at  $300^{\circ}\text{C}$ , plot of hardness, Rockwell Scale "B" as a function of time.

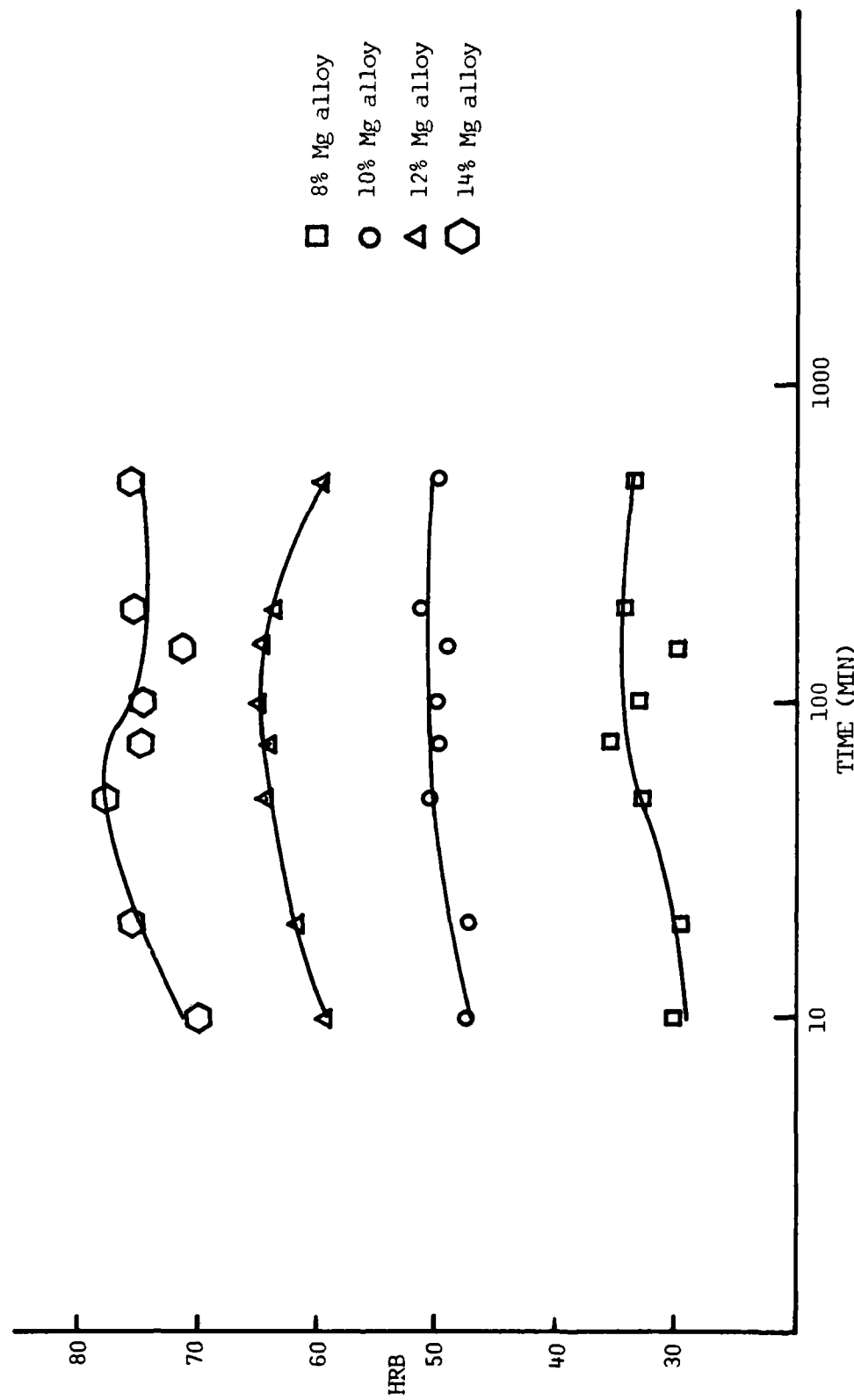


Figure 7. Precipitation Study at  $340^{\circ}\text{C}$ , plot of hardness, Rockwell Scale "B" as a function of time.

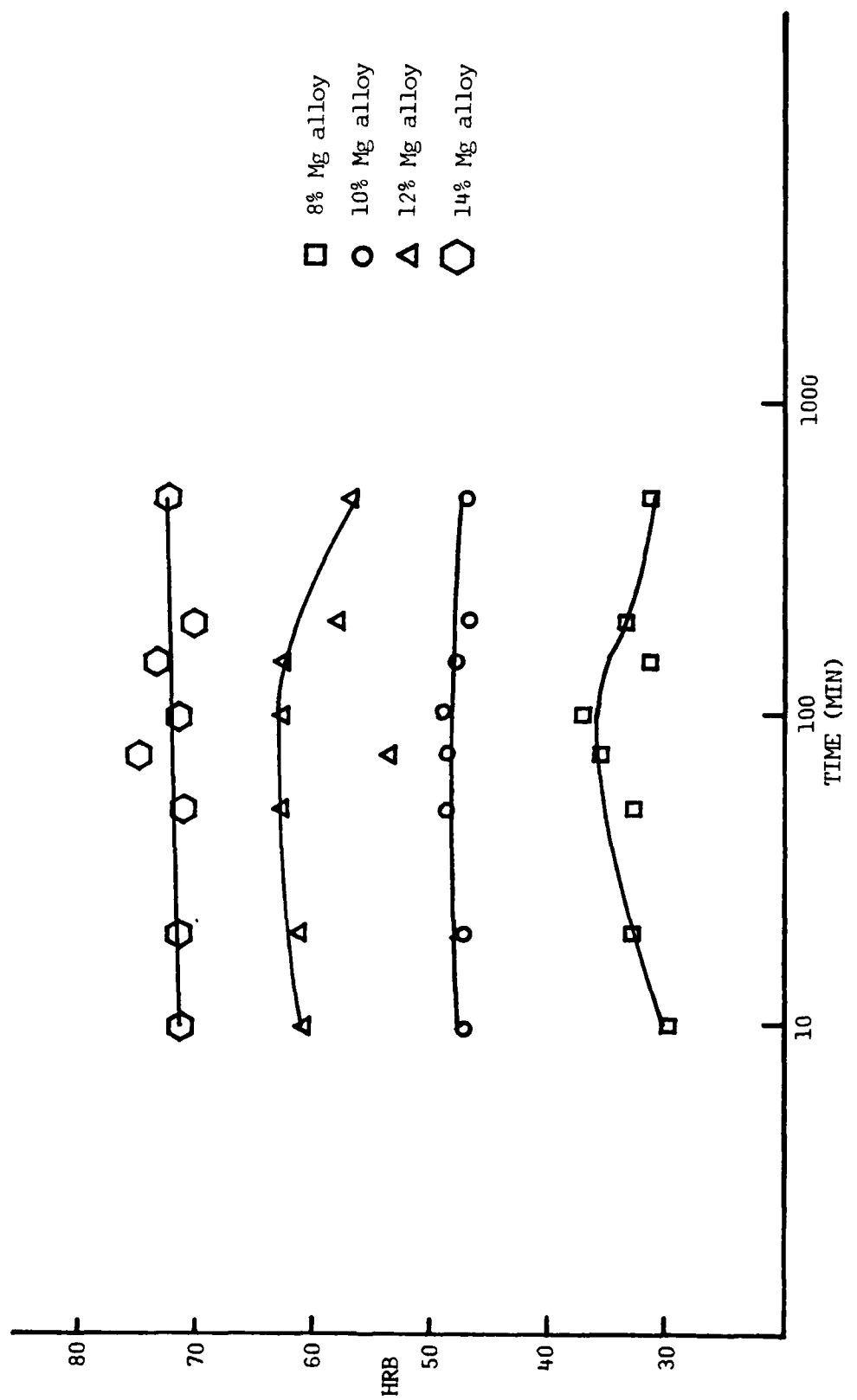


Figure 8. Precipitation Study at  $380^{\circ}\text{C}$ , plot of hardness, Rockwell Scale "B" as a function of time.

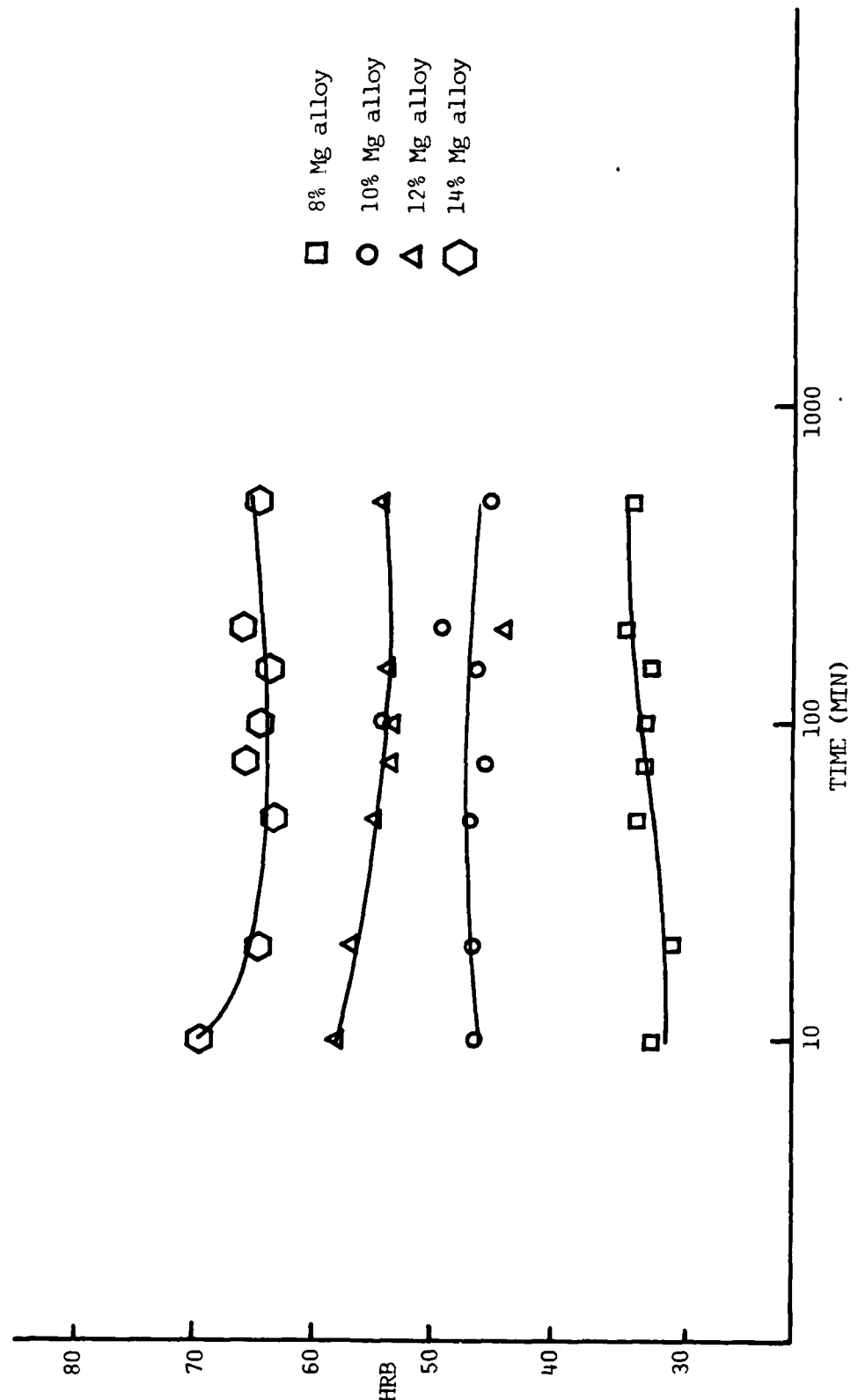


Figure 9. Precipitation Study at  $420^{\circ}\text{C}$ , plot of hardness, Rockwell Scale "B" as a function of time.

The alloys show little change in hardness with annealing time for a temperature of  $380^{\circ}$  C. For a temperature of  $420^{\circ}$  C, the 8% and 10% magnesium alloys show little change in hardness. For the 12% and 14% magnesium alloys there is a gradual decrease in hardness; this temperature is above the solvus for all but the 14% magnesium alloy.

#### C. MICROSTRUCTURE AS A FUNCTION OF TIME AND TEMPERATURE

Figure 10 shows the microstructure of four specimens of the 8% magnesium alloy which experienced fifty minutes at four different temperatures. These micrographs are representative microstructures and it is clearly evident that the precipitation of the intermetallic  $\beta$  phase occurs in the grain boundries.

Figure 11 shows higher magnification micrographs of the grain boundaries for the 8% magnesium alloys that were at temperature for 8 hours and 20 minutes. They show an increase in the amount of precipitation in the interior of the grains that was not evident in the micrographs of Figure 10. Of note is micrograph (c) of Figure 11, which appears to shows a Widmanstätten pattern of precipitation. There is no evidence of either grain growth or recrystallization. It is clearly evident in micrograph (d) of Figure 10 and Figure 11 that the intermetallic  $\beta$  phase has resolved at  $340^{\circ}$  C, a temperature above the solvus temperature for the 8% magnesium alloy.

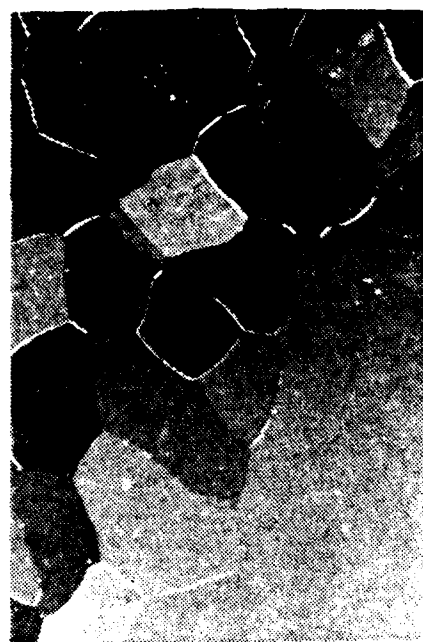
The results of the precipitation study for the 10% magnesium alloy were very similar to that observed for the 8% magnesium alloy. The results for the 12% and 14% magnesium alloy were significantly different. The micrographs of Figure 12



(a)



(b)



(c)

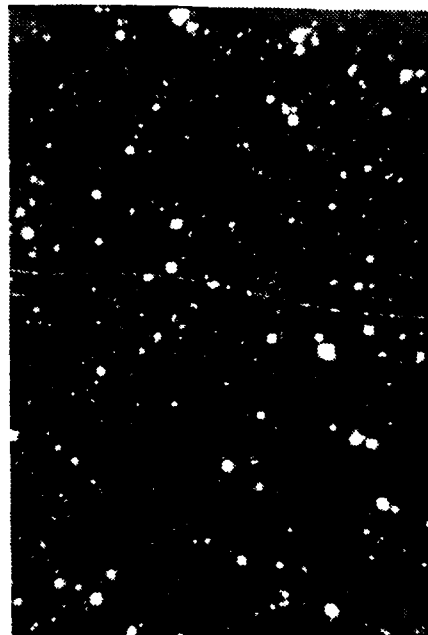


(d)

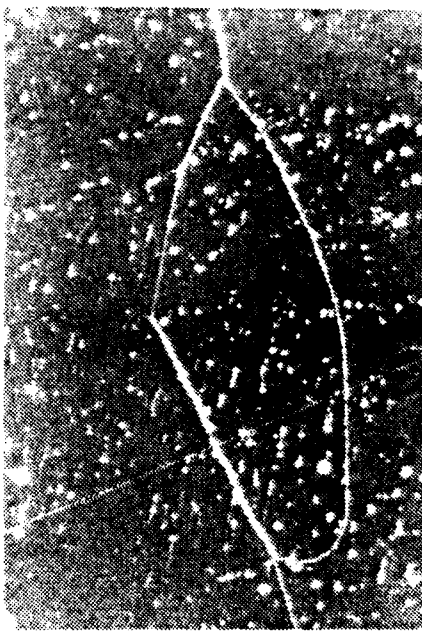
Figure 10. Micrographs (a), (b), (c) and (d) Precipitation Study of 8% Mg alloy, 50 minutes at temperatures  $125^{\circ}\text{ C}$ ,  $200^{\circ}\text{ C}$ ,  $300^{\circ}\text{ C}$ , and  $340^{\circ}\text{ C}$  respectively, 40 X.



(a)



(b)



(c)



(d)

Figure 11. Micrographs (a), (b), (c) and (d) Precipitation Study of 8% Mg alloy, 8 hours and 20 minutes at temperatures  $125^{\circ}\text{C}$ ,  $200^{\circ}\text{C}$ ,  $300^{\circ}\text{C}$ , and  $340^{\circ}\text{C}$  respectively, 160X.



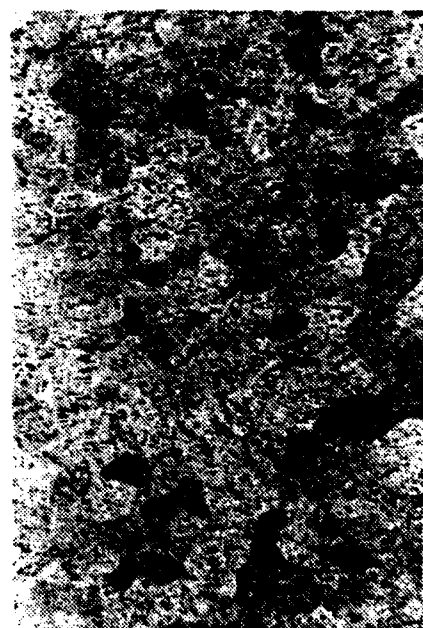
(a)



(b)



(c)



(d)

Figure 12. Micrographs (a) and (c) Precipitation Study of 14% Mg alloy, 20 minutes at temperatures  $125^{\circ}\text{C}$  and  $200^{\circ}\text{C}$  respectively. Micrographs (b) and (d) Precipitation Study of 14% Mg alloy, 50 minutes at temperatures  $125^{\circ}\text{C}$  and  $200^{\circ}\text{C}$  respectively, 40X.

suggest for the 14% magnesium alloy that there is grain growth as well as massive precipitation in the grain boundaries and in the interior of the grains.

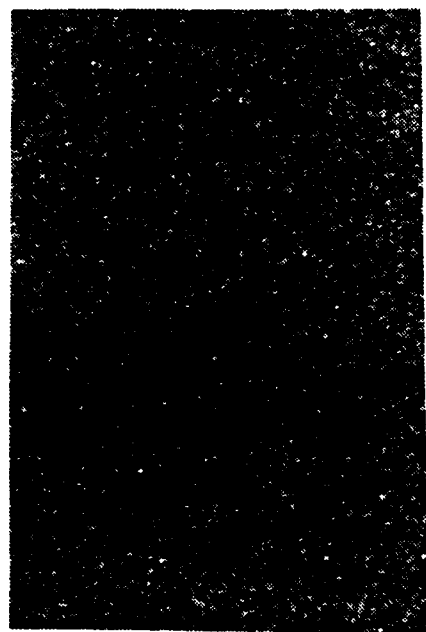
A significant observation is the difference in the location and the form of the precipitation that occurs between 125° C and 200° C. Micrographs (a) and (b) of Figure 12 show that for a temperature of 125° C, there appears to be grain growth and precipitation primarily at the grain boundaries. At 200° C, micrographs (c) and (d) of Figure 12 one can see massive precipitation in what appears to be the former as-cast dendritic sites within the grains and also in the grain boundaries. Micrographs in Figure 13 show the effect of higher temperature, essentially homogenization of the microstructures.

These changes observed in the 14% magnesium alloy show a direct correlation with the hardness exhibited by the alloy at various temperatures. In particular, the pronounced hardness increase seen at 200° C is likely due to fine precipitation. At higher temperatures, where precipitate growth occurs, there is a lesser tendency toward hardening.

#### D. CONCLUSIONS

The precipitation of the intermetallic  $\beta$  phase observed for the 8% and the 10% magnesium alloys occurs primarily in the grain boundaries. The intermetallic  $\beta$  phase that does precipitate in the grain interiors does so on the slip bands.

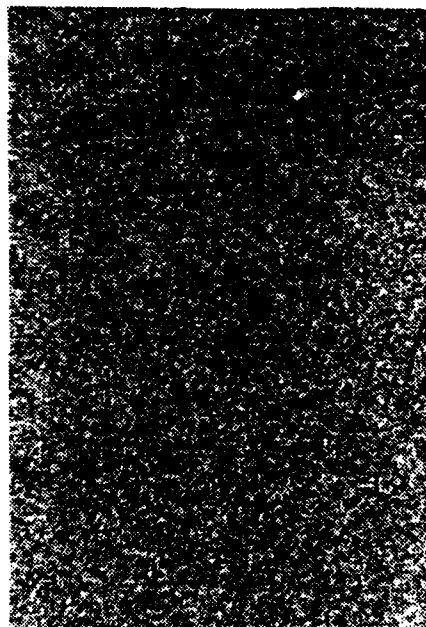
The precipitation of the intermetallic  $\beta$  phase for the 12% and 14% magnesium alloys occurs not only in the grain boundaries



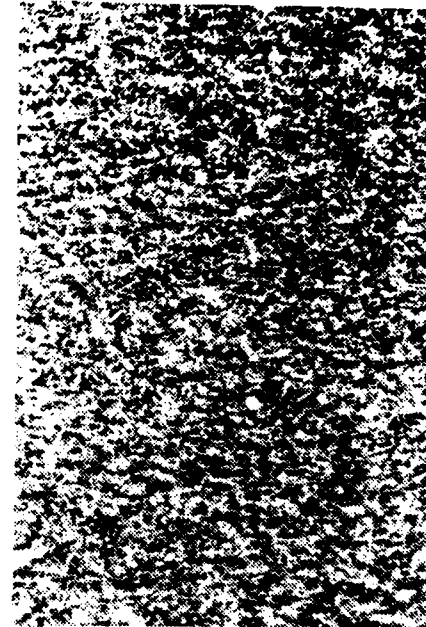
(a)



(b)



(c)



(d)

Figure 13. Micrographs (a) and (b) Precipitation Study of 14% Mg alloy at  $300^{\circ}\text{C}$  for 20 and 50 minutes respectively. Micrographs (c) and (d) Precipitation Study of 14% Mg alloy at  $340^{\circ}\text{C}$  for 20 and 50 minutes respectively, 40X.

but also in the former dendritic sites not completely eliminated by the upset forging and the solution treatment sequence. This massive precipitation of the intermetallic  $\beta$  phase in the grain interiors starts above  $200^{\circ} C$ . The microstructure of the higher temperature and/or prolonged time at temperature samples exhibit a homogeneous structure.

The precipitation study has shown that the alloys will undergo some precipitation hardening and aging, in particular the 12% and 14% magnesium alloys. The study has established the distribution and morphology of the intermetallic  $\beta$  phase.

#### IV. RECRYSTALLIZATION AND RECOVERY IN ALUMINUM-8% MAGNESIUM

##### A. BACKGROUND

In this chapter, the results of a study of recrystallization and recovery in the aluminum-8% magnesium alloy will be presented and discussed. This material was the same as previously discussed in the precipitation study. Recrystallization is the process of formation of new, strain-free grains from an initially strain-hardened structure [Ref. 5]. The process requires diffusion and thus will only occur at elevated temperatures. The important variables are degree of cold work (held constant here), time and temperature.

Usually, recrystallization occurs rapidly only at or above a temperature called the recrystallization temperature. This temperature is typically one-third to one-half the absolute melting temperature of the material; these temperatures are compiled in Table III for the alloys of this study along with data for pure aluminum.

Annealing at temperatures below that sufficient to induce recrystallization will lead to recovery. This process involves rearrangement of dislocation structures produced by prior deformation and is characterized by a decrease in hardness without the formation of new strain-free grains. In the alloys of interest in this work, there is the added factor of precipitation of the intermetallic  $\beta$  phase over the temperature range of interest. This investigation was undertaken to address the question of the effect of precipitation on the recovery/recrystallization process.

Table III  
 Recrystallization Temperatures Calculated for  
 Various High Magnesium Aluminum Alloys  
 (Adapted from Reference 11)

Weight Percent (%)	Melting Temperature (° C)	1/3 T <sub>m</sub> *	1/2 T <sub>m</sub>
0	660	37.9	193.4
8	620	24.5	173.4
10	610	21.2	168.4
12	600	19.6	165.3
14	590	14.6	158.4

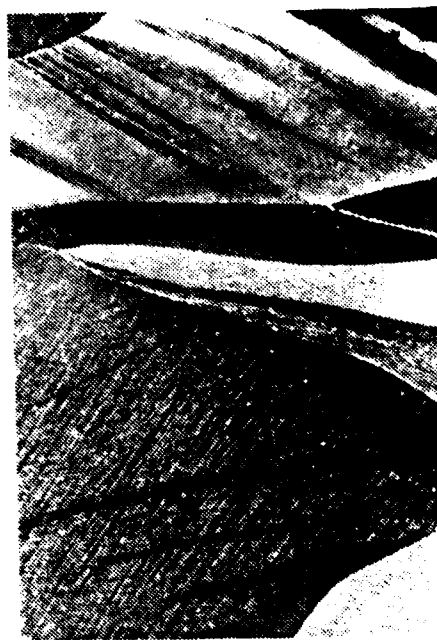
\*T<sub>m</sub> is the temperature in degrees absolute where melting is complete.

## B. PROCEDURE

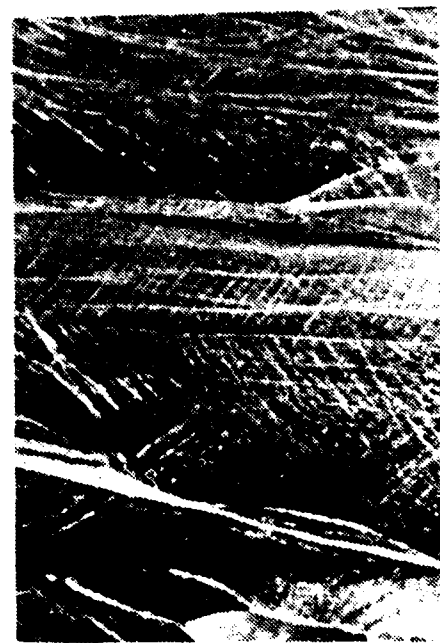
The materials studied were solution treated, forged, solution treated and oil quenched as previously discussed. At this point, they were rolled 50%. One series was cold rolled at  $125^{\circ}$  C, the other at  $20^{\circ}$  C. The series at the higher temperature ( $125^{\circ}$  C) was done because previous work on higher (14% magnesium) magnesium content alloys indicated problems with cracking during rolling at  $25^{\circ}$  C. Rolling at  $125^{\circ}$  C was accomplished by heating to this temperature in a furnace and then rolling the one-inch thick starting billet at a reduction per pass of 0.020 inches with reheating after each pass. Rolling at  $20^{\circ}$  C was accomplished in the same manner except that the material was periodically water cooled to minimize the degree of adiabatic heating during rolling. Small specimens were cut, as before, from the rolled material and annealed and oil quenched. Hardness testing and metallography was done to evaluate the amount of recovery, recrystallization and precipitation that may have occurred.

## C. RESULTS AND DISCUSSION

Metallographic data for the 8% magnesium alloy, rolled at  $125^{\circ}$  C, Figure 14, shows that recrystallization does not occur until  $340^{\circ}$  C is reached. This is substantially above one-half the melting temperature for this alloy and in fact is well above one-half the melting temperature for pure aluminum ( $193.4^{\circ}$  C). However, precipitation occurs up to  $340^{\circ}$  C; this temperature



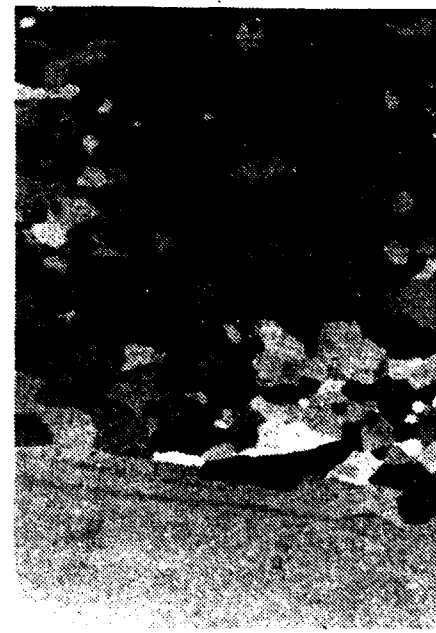
(a)



(b)

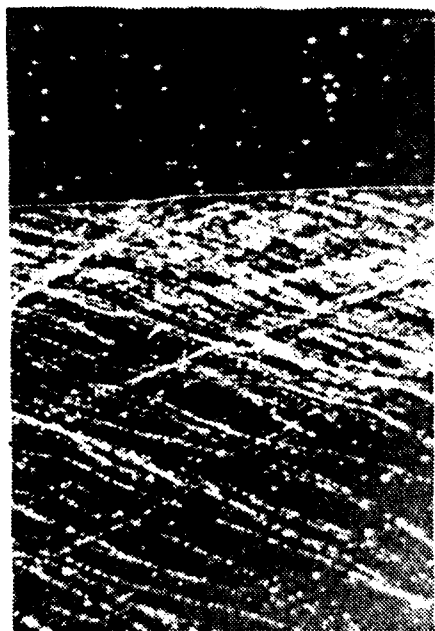


(c)

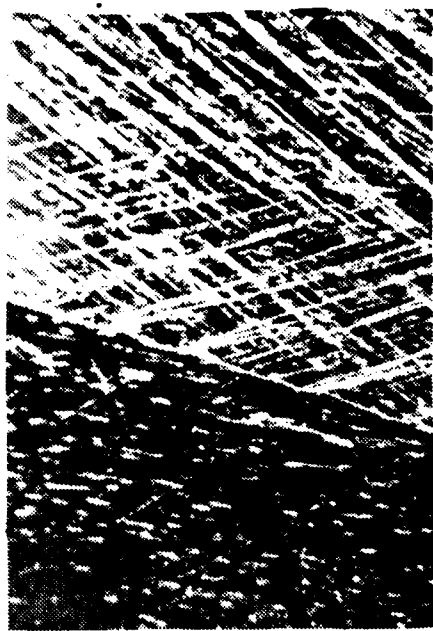


(d)

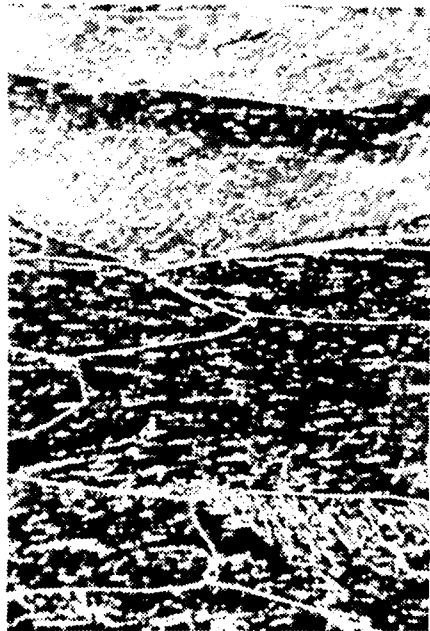
Figure 14. Micrographs (a), (b), (c) and (d) Recrystallization Study of 8% Mg alloy, 50 minutes at temperatures  $125^{\circ}\text{C}$ ,  $200^{\circ}\text{C}$ ,  $300^{\circ}\text{C}$  and  $340^{\circ}\text{C}$  respectively, 40X.



(a)



(b)



(c)



(d)

Figure 15. Micrographs (a), (b), (c) and (d) Recrystallization Study of 8 Mg alloy, 8 hours and 20 minutes at temperatures  $125^{\circ}\text{C}$ ,  $200^{\circ}\text{C}$ ,  $300^{\circ}\text{C}$  respectively, 160X.

is the solvus temperature for this alloy. Precipitation occurs along slip bands and in grain boundaries and appears to occur at an accelerated rate as compared to precipitation without prior cold work (Chapter III). Figure 15 illustrates this further. Figure 16 shows the decrease in hardness as a function of annealing time for the temperature investigated. At and above  $340^{\circ}$  C, the hardness decreases to that of the solution treated condition and recrystallization is complete even in 10 minutes. In contrast, for temperature below this (i.e. below the solvus), hardness decreases to a lesser extent suggesting recovery only is occurring in conjunction with precipitation.

A similar study was conducted with material cold worked at  $20^{\circ}$  C. The as-rolled hardness for this material was higher than that of the material rolled at  $125^{\circ}$  C (Figure 17), but otherwise the same general trends occur. One notable difference is that this material, annealed at  $340^{\circ}$  C, does not soften as rapidly and recrystallize as quickly as the material rolled at  $125^{\circ}$  C. Precipitation occurred in the sample, probably on heating to the annealing temperature, and some time was required to resolution this precipitate prior to the onset of recrystallization. The fully recrystallized condition for this temperature is illustrated in micrographs (a) and (c) of Figure 18 in comparison to the same material annealed at  $380^{\circ}$  C (micrographs (b) and (d) of Figure 18). Figure 19 and Figure 20 illustrate the initial precipitation at  $340^{\circ}$  C.

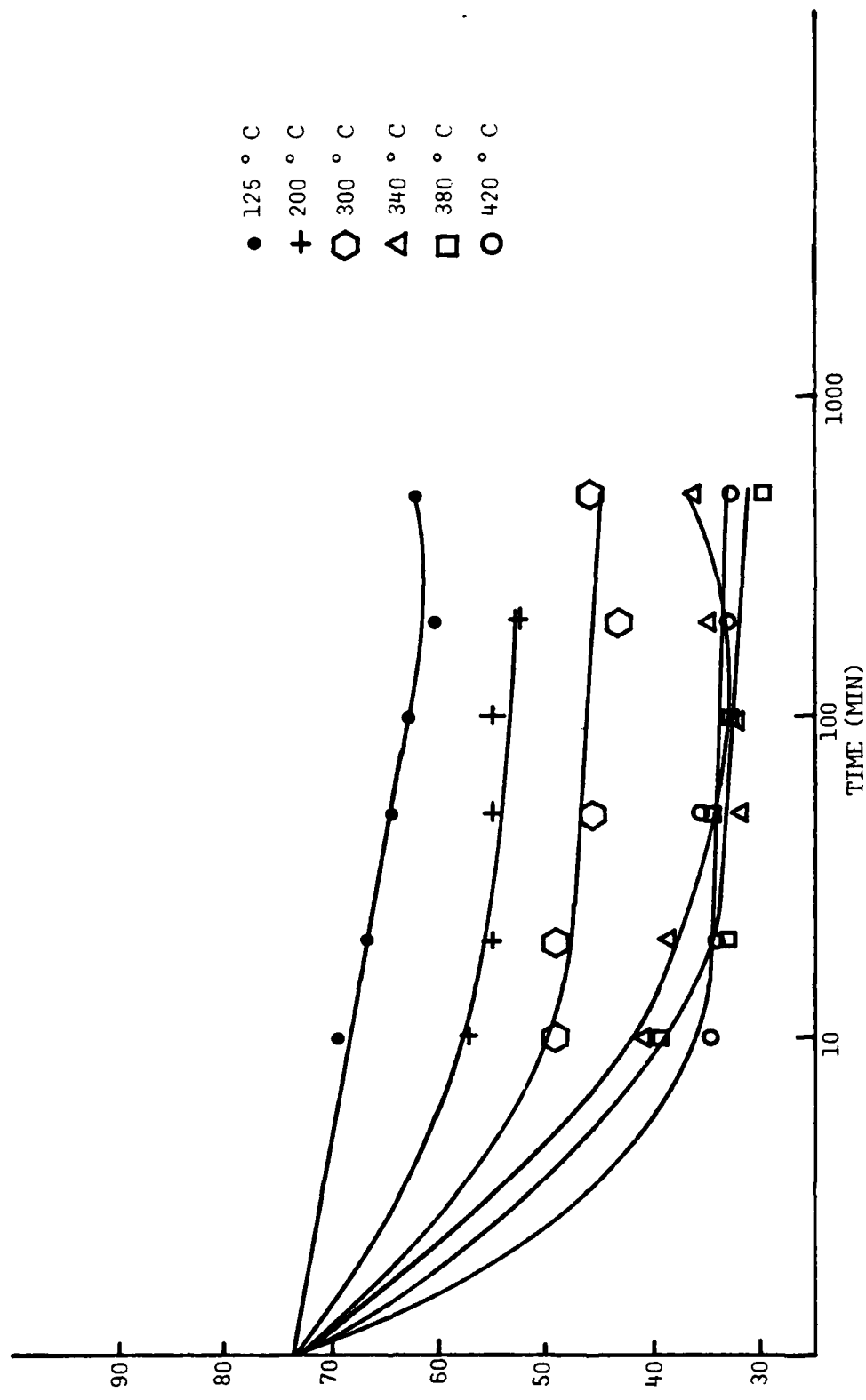


Figure 16. Recrystallization Study of 8% Mg alloy, plot of hardness, Rockwell Scale "B" as a function of time for a deformation temperature of 125°C.

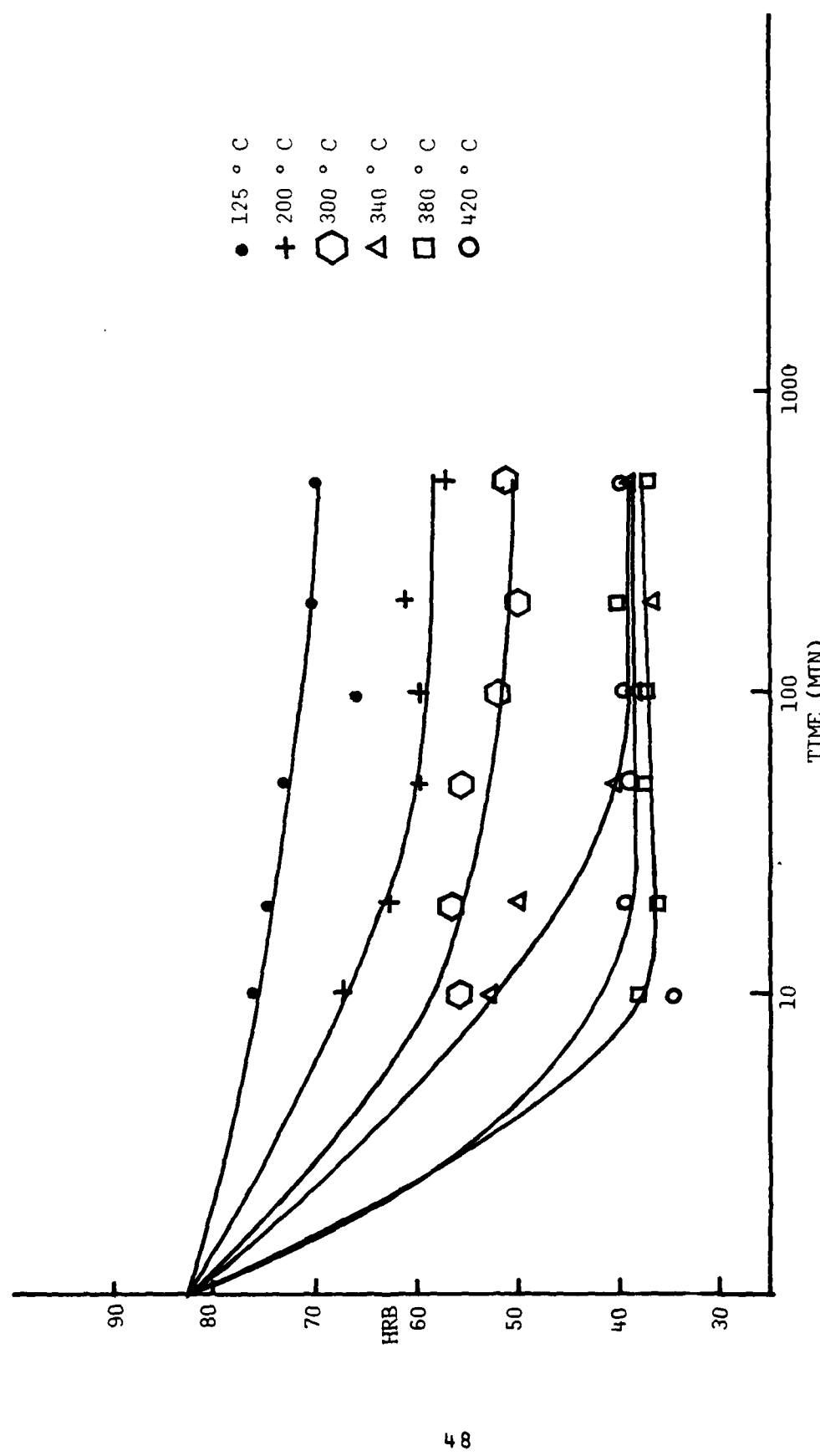


Figure 17. Recrystallization Study of 8% Mg alloy, Plot of hardness, Rockwell Scale "B" as a function of time for a deformation temperature of 20°C.



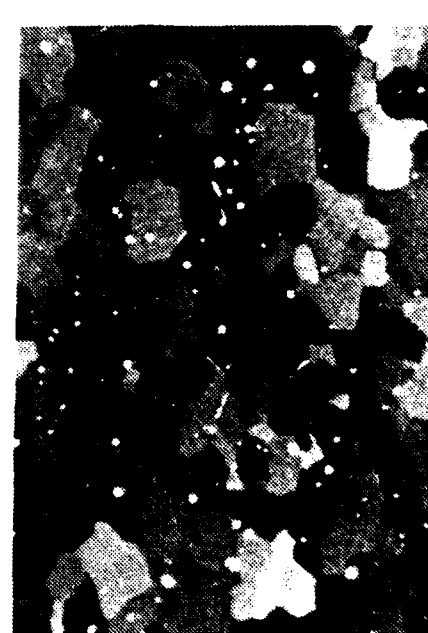
(a)



(b)

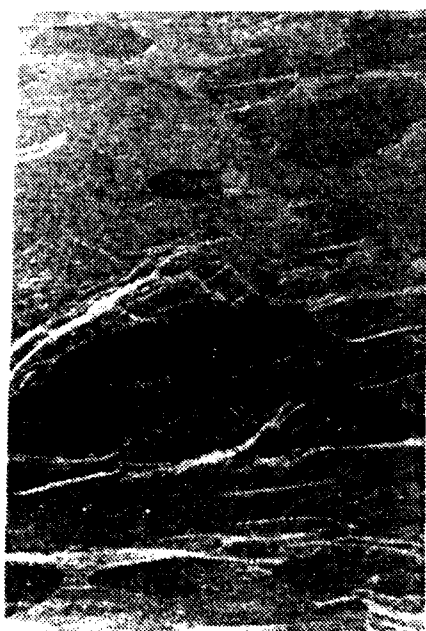


(c)



(d)

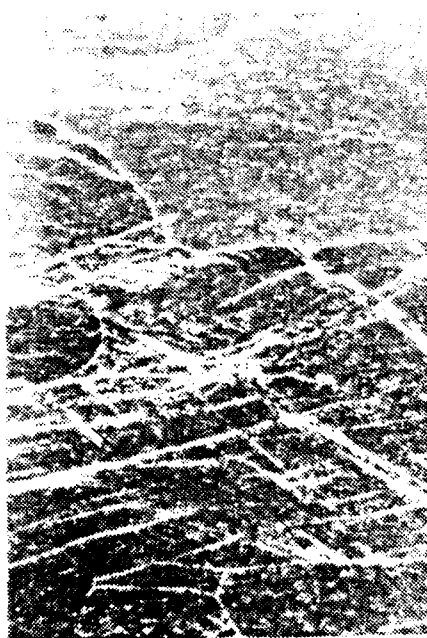
Figure 18. Micrographs (a) and (b) Recrystallization Study of 8% Mg alloy, 8 hours and 20 minutes at 340° C and 380° C respectively, 40X. Micrographs (c) and (d) Recrystallization Study of 8% Mg alloy, 8 hours and 20 minutes at 340° C and 380° C respectively, 160X.



(a)



(b)



(c)



(d)

Figure 19. Micrographs (a) and (b) Recrystallization Study of 8% Mg alloy, at 340 °C for 10 and 50 minutes respectively, 40X. Micrographs (c) and (d) Recrystallization Study of 8% Mg alloy, at 340 °C for 10 and 50 minutes respectively, 160X.



(a)



(b)

Figure 20. Micrographs (a) and (b) Recrystallization Study of 8% Mg alloy, at 340°C for 10 minutes and 1 hour and 40 minutes respectively, 40X.

The significance of these observations is that the process of precipitation in these alloys always precedes - and probably hinders - recrystallization at temperatures below the solvus for the alloy. Recovery and precipitation along slip bands likely relieves stored strain energy reducing the driving force for recrystallization. In contrast, at and above the solvus temperature, precipitation of the intermetallic  $\beta$  phase does not occur and hence recrystallization occurs rapidly. In the previous work Grandon [Ref. 9] and Speed, [Ref. 10] an implied assumption was that recrystallization could occur at such temperatures below the solvus. Were it to occur during rolling, it would lead to refinement of the microstructure and thus enhancement of the subsequent ambient temperature mechanical properties. This study suggests that this is not the case and that grain size refinement is possible only at temperatures above the solvus. This question of precipitation vs. recrystallization during rolling is addressed in the following chapter.

## V. DYNAMIC STUDY OF ALUMINUM-8% MAGNESIUM

### A. BACKGROUND

The investigation described thus far has considered micro-structural changes occurring during annealing of the material. Of primary concern in the program of which this research is a part is the strengthening of these alloys by warm rolling. This means rolling the material at a temperature below the solvus temperature, but at a temperature sufficiently elevated that diffusion, and hence recovery and possibly recrystallization can occur, leading to microstructural refinement. In fact, it was assumed in the work of Grandon [Ref. 9] and Speed [Ref. 10] that recrystallization was possible during rolling under these warm temperature conditions. Thus far, it has been demonstrated that under 'static' conditions (annealing without rolling), recrystallization does not occur at any temperature below the solvus temperature. Instead, precipitation and recovery occur. Recrystallization occurs readily at temperatures equal to or greater than the solvus temperature for the alloy. In this portion of the present investigation, the materials were rolled and the development of the microstructure was followed by periodically sampling the microstructure during rolling. Rolling procedures were structured to allow the material experience varying time at temperature during the rolling process.

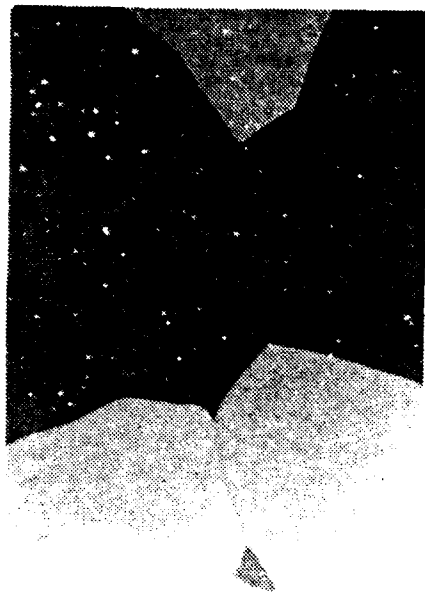
### B. PROCEDURE

The alloy studied here is, again, the same 8% magnesium alloy of the previous portions of this study. Prior processing

consisted of the same solution treatment, forging, solution treatment and oil quenching previously discussed. Three different processing sequences then followed. First, one sample was cold rolled (at 20° C) from an initial thickness of 1.0 inch to a final thickness of 0.070 inch. During this rolling, samples were periodically taken for hardness testing and metallography. Second, samples initially 1.0 inch thick were cold rolled to 50% reduction in thickness and then heated to either 300° C or 340° C and warm rolled to a final thickness of 0.070 inches. This sequence is designated cold/warm. Samples for metallography and hardness testing were taken during these sequences. During the warm rolling stage, the sample was oil quenched, sectioned and then re-heated for further rolling. The third procedure consisted of warm rolling from 1.0 inch to 0.070 inch final thickness at either 300° C or 340° C. To investigate the effect of total time at temperature, reheating times between passes were adjusted to allow samples to experience a total time of either 35, 70 or 210 minutes at temperature during the warm rolling portion of the processing.

#### C. COLD WORKING

The micrographs of Figure 21 and Figure 22 illustrate the progressive change in microstructure during cold rolling of the 8% magnesium alloy. Initially equiaxed grains became elongated; no precipitation or recrystallization occur. Hardness data is presented in Figure 23 for this cold rolling study.



(a)



(b)



(c)



(d)

Figure 21. Micrographs (a), (b), (c) and (d) Dyanmic Study of 8% Mg alloy cold rolling sequence, cumulative rolling strain of .01, .05, .17 and .83 respectively, 40X.



(a)



(b)



(c)

Figure 22. Micrographs (a), (b) and (c) Dynamic Study of 8% Mg alloy cold rolling sequence, cumulative rolling strain of 1.19, 1.85 and 2.36 respectively, 40X.

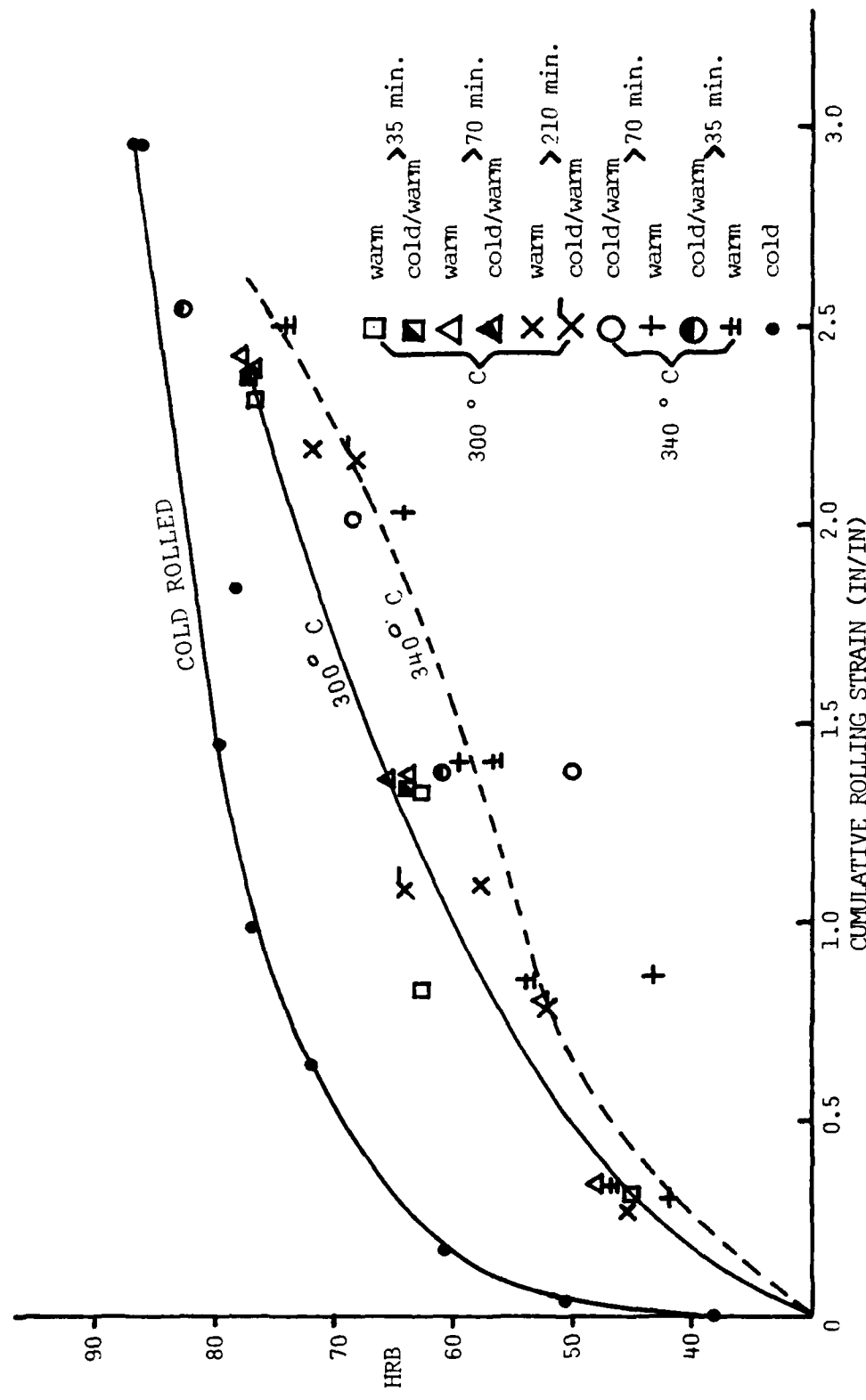


Figure 23. Dynamic Study of 8% Mg alloy, plot of hardness, Rockwell Scale "B" as a function of cumulative strain for cold, cold/warm and warm rolling sequences.

The material is progressively strain hardened from an initial hardness as solution treated of HRB 38 to a final hardness of HRB 90 at the final thickness. The cumulative strain during rolling is defined as  $\epsilon = \ln \frac{l_0}{l_f}$  where  $\epsilon$  is the strain,  $l_0$  is the initial thickness and  $l_f$  is the thickness at the point of hardness measurement. This strain hardening and the accompanying microstructures are characteristic of cold worked materials. It should be noted, however, that an 8% magnesium alloy, with all of the magnesium in solid solution, is metastable at room temperature, i.e. the solid solution is supersaturated. Since ambient temperatures correspond to about 1/3 the melting temperature for aluminum, the possibility exists for precipitation to occur in an uncontrolled manner. Hence the microstructure would be considered unstable.

#### D. COLD ROLLING FOLLOWED BY WARM ROLLING AT 300° C

Micrographs illustrating microstructural changes occurring in these sequences are shown in Figure 24 and Figure 25. During the cold rolling stage, grain elongation occurred as before; upon heating to the warm rolling temperature, in these cases 300° C, precipitation of the intermetallic  $\beta$  phase occurs both in grain boundaries and along slip planes. This precipitation is evident immediately, as before in the study on recrystallization and recovery.

Hardness data (Figure 23) for this sequence shows that hardness increases with rolling strain at this temperature. The metallographic data suggests that precipitation occurs throughout



(a)



(b)

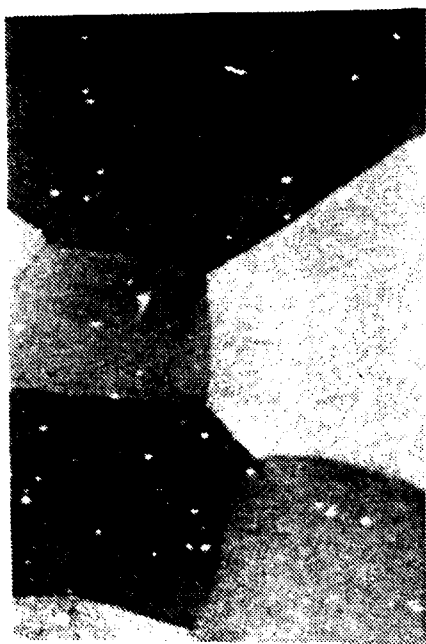


(c)



(d)

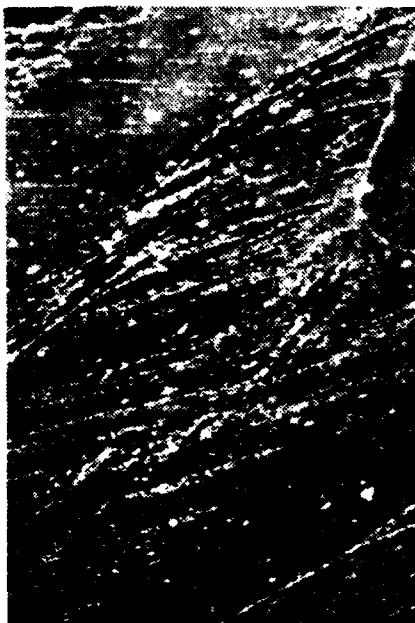
Figure 24. Micrographs (a), (b), and (c) and (d) 300° Dynamic Study of 8% Mg alloy cold/warm rolling sequence, cumulative rolling strain of .33, .78, 1.37 and 2.47 respectively for 70 minutes at temperature, 40X.



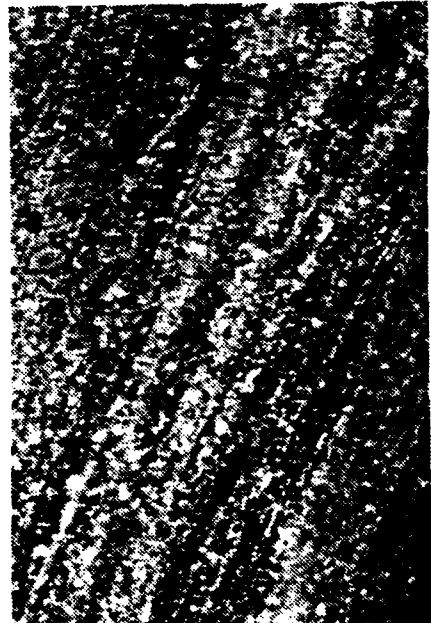
(a)



(b)



(c)



(d)

Figure 25. Micrographs (a), (b), (c) and (d) 300° C Dynamic Study of 8% Mg alloy cold/warm rolling sequence, cumulative rolling strain of .28, .76, 1.08, and 2.16 respectively for 210 minutes at temperature, 40X.

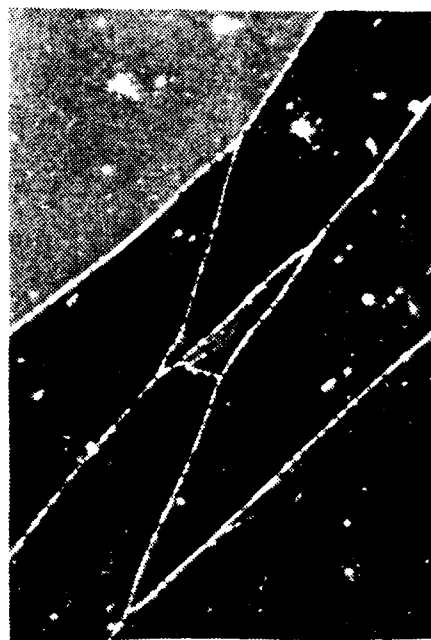
the warm rolling, more uniformly the greater the total time at temperature. As noted previously in the 'static' studies of precipitation, recovery and recrystallization, no recrystallization occurs at this temperature. Instead, the microstructure is dominated by precipitation of the intermetallic  $\beta$  phase. The increase in hardness under these warm rolling conditions as during cold rolling suggests that strengthening is the result of increased dislocation density in conjunction with solid-solution strengthening. The precipitated intermetallic  $\beta$  phase is removing magnesium from solid-solution and recovery (rearrangement of dislocations into more stable, lower energy arrays) is likely occurring, leading to a lesser rate of strain hardening under warm rolling conditions. The precipitated intermetallic  $\beta$  phase may provide some dispersion strengthening as well. Of considerable importance is the potential stability of this structure compared to the unstable structure of the cold rolled material. Precipitation of the intermetallic  $\beta$  phase has occurred in warm rolling which would preclude further uncontrolled precipitation as would be likely to occur for the cold rolled material.

#### E. WARM ROLLING AT $300^{\circ}$ C

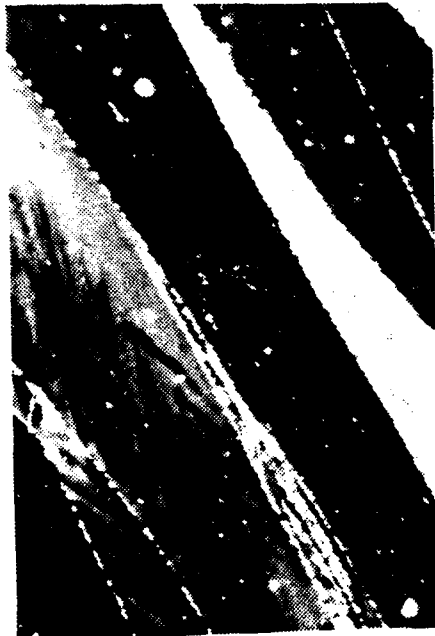
Figure 26 and Figure 27 show micrographs obtained from material experiencing only warm rolling at  $300^{\circ}$  C. Here, precipitation of the intermetallic  $\beta$  phase occurs initially in grain boundaries and as the material is rolled, the precipitate appears to be broken up and dispersed more uniformly in the structure.



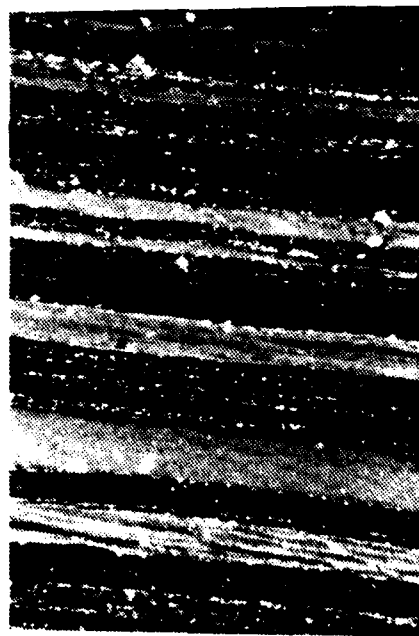
(a)



(b)

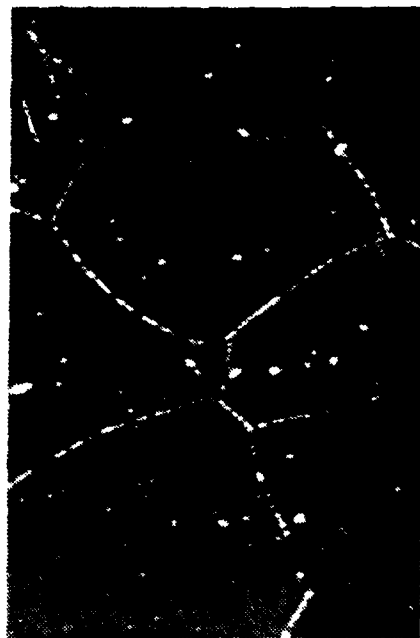


(c)



(d)

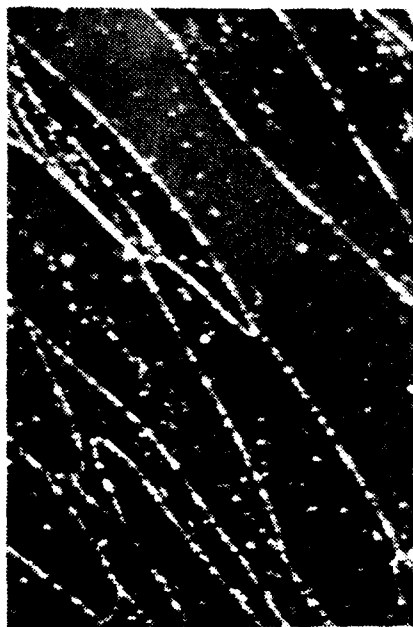
Figure 26. Micrographs (a), (b), (c) and (d) 300° C Dyanmic Study of 8% Mg alloy warm rolling sequence, cumulative rolling strain of .35, .80, 1.37 and 2.45 for 70 minutes at temperature, 40X.



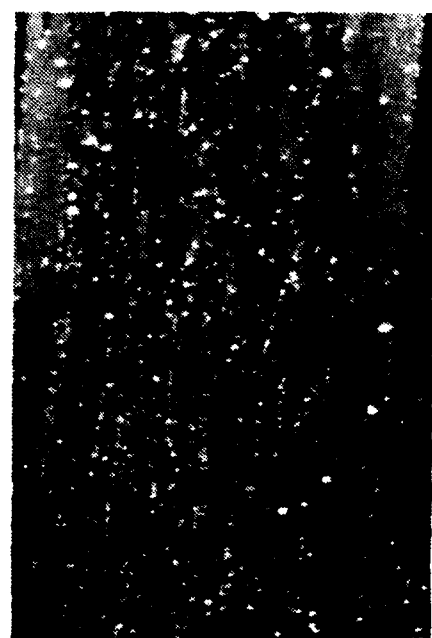
(a)



(b)



(c)



(d)

Figure 27. Micrographs (a), (b), (c) and (d) 300° C Dynamic Study of 8% Mg alloy warm rolling sequence, cumulative rolling strain of .26, .78, 1.08 and 2.19 respectively for 210 minutes at temperature, 40X.

Material receiving the same total deformation but more time at temperature has a more uniform, homogeneous dispersion of the intermetallic phase and perhaps a somewhat less elongated, banded microstructure. Of note is the absence of recrystallization; this rolling temperature,  $300^{\circ}\text{ C}$ , is approximately  $30^{\circ}\text{ C}$  below the solvus temperature for the alloy, yet high in an absolute sense. Still, precipitation occurs and apparently inhibits recrystallization.

#### F. COLD ROLLING FOLLOWED BY WARM ROLLING AND WARM ROLLING AT $340^{\circ}\text{ C}$

This rolling temperature is now essentially at the solvus temperature for the alloy. Micrographs from both cold/warm (Figure 28) and warm (Figure 29) rolling show that recrystallization occurs. In fact, prior cold work leads to a coarser grain size than is attained in the warm worked material. In particular, the micrographs of Figure 29 suggest that recrystallization is complete after a cumulative strain of 2.0 and subsequent elongation of these finer grains is then occurring with further reduction. The hardness of these materials, rolled at  $340^{\circ}\text{ C}$ , increases with strain at a rate only slightly less than that for rolling at  $300^{\circ}\text{ C}$ , Figure 23.

#### G. SUMMARY AND CONCLUSIONS

This 'dynamic' study reaches the same conclusion as the previous 'static' study, namely that recrystallization will occur only at temperatures essentially equal to or greater than the solvus temperature for the alloy. Below the solvus temperature, precipitation and recovery lead recrystallization



(a)



(b)



(c)

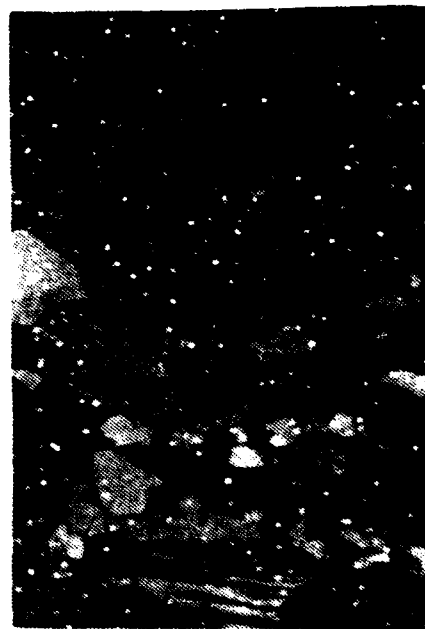


(d)

Figure 28. Micrographs (a), (b), (c) and (d) 340° C Dynamic Study of 8% Mg alloy cold/warm rolling sequence, cumulative rolling strain of .31, .83, 1.39, and 2.02 respectively for 70 minutes at temperature, 40X.



(a)



(b)



(c)



(d)

Figure 29. Micrographs (a), (b), (c) and (d)  $340^{\circ}\text{C}$  Dynamic Study of 8% Mg alloy warm rolling sequence, cumulative rolling strain of .33, .86, 1.4 and 2.03 respectively for 70 minutes at temperature, 40X.

and essentially block its occurrence. The significance of this finding is that recrystallization is not available as a vehicle for microstructural refinement during warm rolling of these alloys. To achieve grain refinement, the material must be hot worked (at a temperature above the solvus temperature) or cold worked and then annealed above the solvus temperature to obtain a fine, recrystallized grain structure.

Strengthening during warm working of these alloys occurs by a mechanism similar to strengthening during normal cold working of a solid solution alloy, i.e. by generation and motion of dislocations, the development of a dislocation sub-structure and by solid solution strengthening. The role of the precipitating intermetallic  $\beta$  phase with regard to strength is not clear. As it forms, magnesium is removed from solid solution. Yet, the precipitated intermetallic  $\beta$  phase, if sufficiently fine, would represent a dispersion of obstacles which should pin and stabilize the dislocation structures formed during rolling.

Mechanical properties attained in the various rolling sequences are given in Table IV. Notable is the high strength of the material given only cold work. Warm worked materials are generally weaker, although they possess a more stable microstructure. It should be noted that prior work by both Grandon and Speed indicates that both higher strengths and higher ductilities are attainable in alloys containing 10% magnesium (vs. the 8% magnesium of this study). This study

has focused on the 8% magnesium alloy for reasons of experimental simplicity. Yet the same conclusions appear to be applicable to the 10% magnesium alloys, based on examination of the data of Grandon [Ref. 9] and Speed [Ref. 10].

Table IV  
 Table of Thermomechanical Processing Mechanical Testing Results  
 (8% Magnesium Alloy)

	Ultimate Tensile Strength, psi (MPa)		0.2% Offset Yield Strength, psi (MPa)		Elonga- tion, %
Cold Rolled	80,000 (551.2)		67,000 (461.6)		6.6
Cold/Warm Rolled (300° C)					
35 Min	61,400 (423.0)		47,900 (330.0)		8.5
70 Min	64,200 (442.3)		52,400 (361.0)		8.5
Cold/Warm Rolled (340° C)					
35 Min	59,700 (411.8)		46,800 (322.4)		9.0
70 Min	— —		— —		— —
Warm Rolled (300° C)					
35 Min	59,400 (409.2)		49,500 (341.10)		8.0
70 Min	59,700 (411.3)		47,800 (329.3)		9.0
Warm Rolled (340° C)		—			
35 Min	59.500 (412.7)		46,800 (322.4)		10.0
70 Min	— —		— —		— —

## VI. CONCLUSIONS AND RECOMMENDATIONS

This study has shown that recrystallization for these alloys will not occur below the solvus temperature for material with either prior cold work, or material isothermally warm worked. An understanding of this result may enable one to achieve better homogenization of the alloys leading to improved tensile properties with these alloys relative to those of non-heat treatable aluminum alloys commercially available.

Further studies of high magnesium alloys should be directed to the following areas:

1. Precipitation and recrystallization studies of the high magnesium alloys not covered by this work and new alloys that have additions of copper and manganese as precipitate inhibitors and grain refiners.
2. A scheme of thermomechanical processing that has a recrystallization stage after the forging and prior to the warm rolling sequence.
3. A study of the fatigue and corrosion properties of those alloys that display superior tensile properties.

## LIST OF REFERENCES

1. Source Book on Selection and Fabrication of Aluminum Alloys, 1st ed., p. 1-20, American Society of Metals.
2. Brick, R. M., Pense, A. W., Gordon, R. B., Structure and Properties of Engineering Materials, 4th ed., p. 186-193, McGraw-Hill, 1977.
3. Introductory Welding Metallurgy, 1st ed., p. 60-66, American Welding Society.
4. Van Vlack, L. H., Elements of Materials Science, 2nd ed., p. 220-277, 429-431, Addison-Wesley, 1964.
5. Reed-Hill, R. E., Physical Metallurgy Principles, 2nd ed., p. 358-375, D. Van Nostrand, 1973.
6. Ness, F. G., Jr., High Strength to Weight Aluminum-18 Weight Percent Magnesium Alloy Through Thermal Mechanical Processing, M. S. Thesis, Naval Postgraduate School, Monterey, California, December 1976.
7. Bingay, C. P., Microstructural Response of Aluminum-Magnesium Alloys to Thermomechanical Processing, M. S. Thesis, Naval Postgraduate School, Monterey, California, December 1977.
8. Glover, T. L., Effects of Thermo-Mechanical Processing of Aluminum-Magnesium Alloys Containing High Weight Percent Magnesium, M. S. Thesis, Naval Postgraduate School, Monterey, California, December 1977.
9. Grandon, R. A., High Strength Aluminum-Magnesium Alloys: Thermomechanical Processing, Microstructure and Tensile Mechanical Properties, M. S. Thesis, Naval Postgraduate School, Monterey, California, March 1979.
10. Speed, W. G., An Investigation into the Influence of Thermo-mechanical Processing on Microstructural and Mechanical Properties of High-Strength Aluminum-Magnesium Alloys, M. S. Thesis, Naval Postgraduate School, Monterey, California, December 1979.
11. Metals Handbook, 8th ed., U. 8, p. 261, American Society of Metals, 1973.

## INITIAL DISTRIBUTION LIST

No. Copies

1. Defense Documentation Center Cameron Station Alexandria, Virginia 22314	2
2. Library, Code 0142 Naval Postgraduate School Monterey, California 93940	2
3. Department Chairman, Code 69Mx Department of Mechanical Engineering Naval Postgraduate School Monterey, California 93940	1
4. Professor T. R. McNelley, Code 69Mc Department of Mechanical Engineering Naval Postgraduate School Monterey, California 93940	5
5. LT Charles W. Chesterman, Jr., USN 721 Claret South Calistoga, California 94515	2